**Insights into Conformational Ensembles of Compositionally Identical
Disordered Peptidomimetics**

Erin C. Day, Keila C. Cunha, Roy J. Zhao, Audra J. DeStefano, James N. Dodds, Melissa A. Yu, Jaina R. Bemis, Songi Han, Erin S. Baker, Joan-Emma Shea, Rebecca B. Berlow, Abigail S. Knight*

Department of Chemistry, The University of North Carolina at Chapel Hill

aknight@unc.edu

## *Supporting Information*

## Materials and Instrumentation

*Materials:* All chemicals were of analytical purity grade and used as obtained unless otherwise specified. *N,N'*-diisopropylcarbodiimide (DIC, >99%) was purchased from Oakwood Products. Dichloromethane (DCM), dimethyl sulfoxide (DMSO), acetone, ethanol anhydrous (≥99.5%, 200 proof), sodium hydroxide, acetonitrile (ACN, HPLC grade), sodium phosphate dibasic heptahydrate, hydrazinium hydroxide (≥98%), and formic acid (LC-MS grade) were purchased from Fisher Scientific. 4-Amino-TEMPO (98%) was purchased from AmBeed. 4-Methylpiperadine was purchased from TCI Chemicals. Rink amide PEGA resin, HMBA PEGA resin, *N,N*-diisopropylethylamine (DIPEA, 99%), *n*-butylamine (99.5%), trifluoroacetic acid (TFA, 99%), triisopropylsilane (TIPS), 4-(2-hydroxyethyl)piperazine-1-ethanesulfonic acid (HEPES ≥99.5%), 4-amino-2,6-diphenylphenol (98%), 2,4,6-triphenylpyrylium tetrafluoroborate (98%), alpha-cyano-4-hydroxycinnamic acid (99%), *N,N*-dimethylformamide (DMF), ammonium phosphate monobasic (98.5%), sodium trifluoroacetate (NaTFA, 98%), and rink amide polystyrene resin were purchased from Sigma Aldrich. Sodium acetate anhydrous (99.995%) was purchased from VWR. Fmoc-glycine and *O*-(1H-6-Chlorobenzotriazole-1-yl)-1,1,3,3-tetramethyluronium (HCTU) were purchase from ChemImpex. All NMR solvents were purchased from Cambridge Isotope Laboratories. Bromoacetic acid was purchased from ChemImpex and re-crystallized in high-boiling (60-80 °C) petroleum ether and stored in desiccator. Water (ddH$_2$O) used in these experiments was purified to a resistivity of 18.2 MΩ·cm (at 20.5 °C) using an ultrapure water purification system from Milli-Q Gradient (Millipore) and Atrium Mini (Sartorius).

*Instrumentation:* Samples were centrifuged using a Thermo Scientific Heraeus Multifuge X3R Refrigerated Centrifuge, Thermo Scientific Heraeus Pico 21 Microcentrifuge, or a Thermo Scientific mySPIN 6 Mini Centrifuge depending on total volume. Samples of low volume (<1.5 mL) were dried on CentriVap centrifugal concentrator with glass lid equipped with acid-resistant components coupled to FreeZone benchtop freeze dryer (2.5 L, -84 ºC; Labconco). $^1$H-nuclear magnetic resonance (NMR) spectra were recorded on a Varian VNMRS 600 (150) MHz spectrometer. Using Shimadzu liquid chromatograph single quadrupole mass spectrometer (LCMS 2020), samples analyzed and purified on C18 columns, a Shimadzu Nexcol C18 5 μm (50 × 3.0 mm) column or a Phenomenex Aeris Peptide (100 × 4.6 mm) and Semiprep Restek C18 (250 × 10 mm), respectively. The flow rate was set to 0.4 mL/min for analytical runs and 4.0 mL/min for purification RP-HPLC runs. A solvent system of water + 0.1% formic acid (solvent A) and acetonitrile + 0.1% formic acid (solvent B) was used for gradient elution. Acetonitrile (Fisher Scientific, Optima grade, 99.9%) and formic acid (Fisher Scientific, 99+%) were used to prepare mobile phase solvents. Eluted peaks were detected by absorbance at 218 nm. All data were visualized with Shimadzu LabSolutions software.

## Synthesis and Experimental Procedures
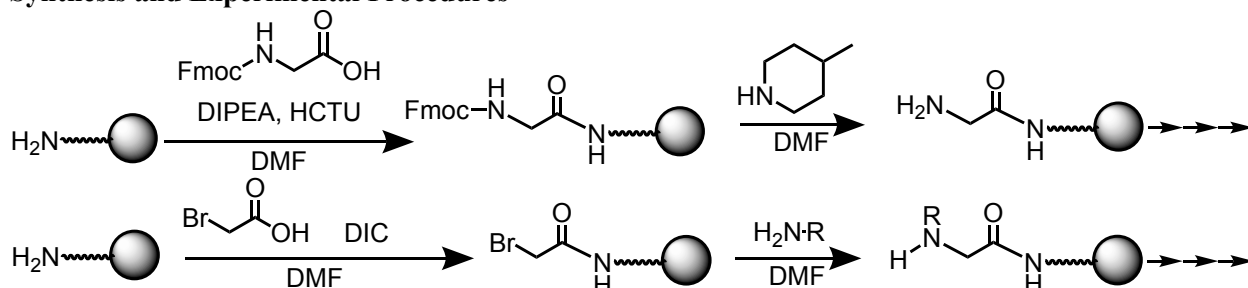


**Peptoid and peptide (N-substituted Glycine Oligomer) Synthesis[1,2]:** Peptidomimetic synthesis was performed at room temperature performed on a Liberty Blue peptide synthesizer (CEM Corporation, Matthews, NC). Peptoids and peptides to be screened by immobilized aqueous assays were synthesized on rink-amide PEGA hydroxymethylbenzoic acid (HMBA) PEGA resins (0.37 meq/g, Novabiochem – Merck Millipore),  respectively Peptoids synthesized on a large scale (0.05 mmol) for solution assays were synthesized on rink amide polystyrene resin (0.51 meq/g, ChemImpex). Reaction conditions and equivalents were used as described below.

| Macromolecule synthesis step | Step | Rxn Time | Reagent | Eq. | Conc. in DMF of stock |
|---|---|---|---|---|---|
| Fmoc-protected amino acids | Deprotection | 20 min | 4-Methylpiperdine | Excess (1 mL / 0.025 mmol of resin) | 20% |
| | Coupling** | 20 min | Fmoc-glycine | 10 | 0.3 M |
| | | | HCTU | 10 | 0.3 M |
| | | | DIPEA | 20 | 0.6 M |
| Peptoid monomer coupling | Coupling (acylation) | 30 min | Bromoacetic acid | 16 | 0.8 M |
| | | | DIC | 16 | 0.8 M |
| | Displacement | 1 h | *n*-butylamime | 20 | 2.0 M |
| | | 1 h | 4-amino-TEMPO | 50 | 1 M (in NMP) |
| Cleaving cocktail | Acid cleaving | 2-3 h for large cleave | Trifluoroacetic acid | Excess (1 mL / 0.01 mmol of resin) | 95% |
| | | | Water | | 2.5% |
| | | | Triisopropylsilane | | 2.5% |

**Cleavage from Rink Amide PEGA and Standard Rink Amide PS-core Resins:** Peptoid samples were cleaved from rink amide resins using with standard cleaving cocktail (95/2.5/2.5 TFA/$H_2O$/TIPS).

| *Rink amide resin* | *Amount* | *Volume of cocktail* | *Reaction time* |
|---|---|---|---|
| Standard | 25-50 mg | 12 mL | 3 hours |
| Standard | <1 mg | 1 mL | 30 min |
| PEGA | 1-2 mg | 1 mL | 30 min |

*HMBA resin*

**First residue coupling to hydroxymethylbenzoic acid resin (HMBA-PEGA)**
HMBA-PEGA resin (100 mg) was swelled in DCM for 30 min and rinsed with DMF × 3. On ice, 4.0 mL of 0.2 M Fmoc-Lys(boc) (20 eq) with 62 µL DIC (10 eq) were chilled for 20 min. The Fmoc-AA and DIC mixture was added to the swollen resin, followed by 40 µL of DMAP in DMF (0.2 eq). The reaction was warmed to room temperature as it stirred for an hour. After rinsing with DMF × 3, subsequent reactions proceeded using standard peptide and peptidomimetic synthesis described above.

**Sidechain deprotection**
To remove acid labile protecting groups on the amino acids (e.g., tBu), samples were incubated with 4 mL of TFA cocktail (95/2.5/2.5 TFA/$H_2O$/TIPS) for 30 min. Substantially longer reaction times began to degrade the resin.

**Cleaving from HMBA resin**
In dioxane, resin (~1 mg) was swelled for 30 min. For 20 min, a 3:1 mixture of dioxane:100 mM NaOH (final concentration 25 mM NaOH) was chilled on ice. The base mixture (1 mL) was added to the drained swollen resin. Reaction warmed to room temperature as it stirred for 20 min. The samples were drained into 250 µL 0.1 M HCl on ice. The cleaved material was then dried on Centrivap and prepped for LC-MS.

**MALDI-TOF Analysis:** A 10 mg/mL solution of α-cyano-4-hydroxycinnamic acid was prepared by dissolving the matrix (20 mg) in water/ACN (50/50, 2.0 mL) with 0.1% TFA (2.0 µL) and ammonium phosphate (20 µL of a 0.6 M aq solution). The final matrix was prepared by mixing 900 µL of the α-cyano-4-hydroxycinnamic acid solution with 100 µL of NaTFA solution (10 mg/mL in 50/50 water/ACN), and frozen in 30 µL aliquots to thaw as needed. Peptidomimetic samples were dissolved in 1.0 µL matrix solution and spotted directly onto an Applied Biosystems 384 Opti-TOF 123 × 81 mm stainless-steel plate. Additional 0.5 µL of matrix was spotted on top of samples to improve spot crystallization quality as needed. MALDI spectra were collected on an AB Sciex 5800 MALDI-TOF/TOF.

**Molecular Dynamics Simulations**
**System Parameters and Preparation:** The Molecular Dynamics (MD) simulations were performed with GROMACS2019.6[3] and a forcefield adapted for the target peptoid sequences. We started from each sequence extended in a cubic simulation box with dimensions 6nm × 6nm × 6nm, solvated with SPC water molecules[4]. One water molecule in each system was substituted with a Cl⁻ ion to obtain an overall neutral system.

After solvation, the energy for each system was minimized with the steepest descent method considering a step size of 0.01 ns. We concluded the minimization when the maximum force is under the threshold of $< 1000$ kJ/mol$^{-1}$nm$^{-1}$. If this limit was not met, as it was often the case for the simulated sequences, we dictated a maximum number of energy-minimizing steps to be 50000. Periodic boundary conditions were applied in all three dimensions.

Afterwards, the entire systems were linearly heated to a reference temperature of 300 K for 1 ns with a velocity-rescaling[5] thermostat and 0.1 ps time constant. For accuracy, two coupling groups of solvent and peptoid were separately treated. An NVT ensemble was used for these simulations with periodic boundary conditions in all x, y, z directions. During the simulations, we used a leapfrog algorithm[10] with a step size of 2 fs to integrate the Newtonian equation of motion. The center of mass translation was removed at the frequency of 100 steps. This step also included a position restraint on the heavy atoms of peptoids, under a force of 1000 kJ/mol$^{-1}$nm$^2$ in all directions. Moreover, we constrained all bonded interactions using the LINCS method.[6] For the electro[9]static interaction, we applied the particle mesh Ewald (PME) summation[7] in Fourier space for long-range interactions where the cutoff range was larger than 1.0 nm, while we calculated the short-range electrostatic and van der Waals interactions directly. Overall, we applied a Verlet cutoff scheme[8] to locate neighboring atoms and calculate their interactions, with the information for non-bonded pairs updated at every 10 steps. Other run parameters not specified here were used with the Gromacs default values. Following this temperature equilibration step, we lastly equilibrated the system's pressure by performing a 20 ns NPT simulation free of position restraints. The pressure equilibration was performed under an isotropically-coupled Berendsen barostat[9] at the reference pressure of 1 bar, with a time constant of 0.5 ps and compressibility of $4.5 \times 10^{-5}$ bar$^{-1}$ for each bulk water simulation. All the other simulation conditions were the same as described above.

**Molecular Dynamics Simulations: Replica-Exchange Molecular Dynamics (REMD) Simulations:** We used the resulting systems after the NPT equilibration to create replicas for our REMD simulation. We established 64 replicas, with their temperature ranging from 295 K to 517 K. Each replica was heated from 300 K to its target temperature during a 10 ns NVT simulation, using the same run parameters described in the NVT step above, but without position restraints. These temperatures were optimized so that the exchange rate between neighboring replicas was approximated 25% from running the REMD simulation for 10 ns. All replicas then underwent the production REMD simulations for 600 ns under an NVT ensemble and using the Nosé-Hoover thermostat[5] with 1 ps time constant, with the attempt to exchange replicas every 3 ps. The frequency for center of mass motion removal was updated every 500 steps. Other run parameters were the same as in the previous step. The coordinates from each trajectory were saved at every 10 ps. Furthermore, the first 100 ns of REMD was neglected to ensure that the harvested trajectories were sufficiently equilibrated. All the simulation results presented are solely from the 500 ns following this neglected portion, which gives a total of 50,000 steps analyzed from each system.

**Molecular Dynamics Simulations: Analysis Tools:** We used of the following GROMACS analysis tools: *hbond*, to count the number of hydrogen bonds with a 3.5 Å donor-receptor distance cutoff and a 30-degree angle (Hydrogen - Donor - Acceptor); *gyrate*, to compute the radii of gyration of the sequences; *pairdist*, to measure the distance between the two farthest atoms, which is the maximum distance inside the molecule; *distance*, to measure the distance between two designated residuals' center of mass (which we use to measure the distance between the two ending terminal groups); *cluster*, to sample and group the nonterminal backbone structures of the sequences within an RMSD cutoff of 1.4 Å, using the Daura algorithm. To further validate the clustering results, we performed additional clustering analysis for all sequences using a shorter RMSD cutoff (1.0Å) and different calculation methods (GROMOS, Linkage, and Jarvis-Patrick) implemented in GROMACS. The results are presented in Table S3. Each ordered pair in a given cell indicates first the number of frames in the most abundant cluster, followed by the total number of clusters. Though the number of clusters remains high for all sequences, a decreasing trend of dib > r2 > r1 > alt is evident across different clustering methods. The new clustering analysis confirms our conclusion regarding using number of clusters as a proxy for conformation disorder.

**LC-IMS-MS Methods:** Samples were prepared at 10 µM in 50/50 MeOH/water with 0.1% formic acid and heated at 37°C overnight before running. Peptoids were profiled by liquid chromatography, ion mobility, and mass spectrometry (LC-IMS-MS) to assess complementary separation mechanisms and facilitate characterization of peptide sequence variation. Samples were diluted to a working concentration of 10 µg/mL and injected onto an Agilent 1290 LC system for chromatographic separation on a Restek Raptor C18 column (1.8 µm, 50 mm × 2.1 m, P/N: 9304252) prior to IMS-MS analysis performed on the Agilent 6560 IM-QTOF platform, which has been characterized previously.[11,12] For gradient methods and extended chromatographic parameters, see **Figure S8**. Following chromatographic separation, analytes were ionized via electrospray ionization (ESI) in positive mode and mobility separated in the uniform field drift tube prior to mass analysis. Peptides formed both singly charged and doubly charged species $[M+H]^+$ and $[M+2H]^{2+}$, however the doubly charged adducts provided significantly greater signal and hence were prioritized in subsequent data analysis. Raw drift times were converted to collision cross section values (CCS) using the well-characterized single-field method,[13,14] wherein a set of known calibrant ions (here, Agilent Tune Mix) are analyzed with previously measured CCS values and the observed experimental drift times are used to create a calibration curve relating CCS to measured drift time, and subsequently measured peptide drift times are converted to CCS values.

**NMR:** NMR samples were prepared at a concentration of 0.5 mM in 50 mM sodium acetate pH 4.5 with 1% $D_2O$ and heated at 37°C overnight before running. All NMR experiments were carried out at 298K on a 600 MHz Bruker Avance III HD spectrometer equipped with a cryoprobe. One dimensional $^1H$ NMR spectra were collected using the standard Bruker pulse sequence 'zgesgp' with 32678 points, a spectral width of 9615 Hz (16 ppm), and 64 scans. Spectra were processed and analyzed using MNova (Mestrelab) on NMRbox.[15] DOSY data were collected using the standard Bruker pulse sequence 'stebpgp1s19' with 16384 points and a spectral width of 7212 Hz (12 ppm) in the direct dimension, a diffusion delay of 100 ms, a bipolar gradient pulse length of 3 ms, and 16 gradient strengths incremented linearly from 2.4 to 45.7 G/cm. Each spectrum in the DOSY array was measured with 128 scans. DOSY data were processed and analyzed using the GNAT software package[16],[2] installed on NMRbox.[15] Diffusion coefficients (D) were calculated for peaks in the amide region of the spectrum (6.5 – 9 ppm) by monoexponential fitting to the Stejskal-Tanner equation.[17,18]

**Radical Regeneration of TEMPO 20mers:** Because nitroxide radicals are disproportionated during TFA cleavage, spin-labeled polypeptoids are subjected to ammonia treatment to partially regenerate the radicals. Radicals were regenerated by rigorous mixing in a 7 N ammonia in methanol : water (9:1). After 4 hours of mixing, the solution was removed under vacuum and the peptoids were lyophilized from acetonitrile and water.

**DEER Measurement of P(R$_{ee}$):** Samples were dissolved in 70/30 v/v $D_2O$/d-glycerol at a concentration of 200 µM and 30 µL of this solution is loaded into a 3 mm OD, 2 mm ID quartz tube. Liquid nitrogen was used to flash freeze samples immediately prior to the DEER experiment. Sample temperature was held at 60 K for the duration of the experiment using a Bruker/ColdEdge FlexLine Cryostat (Model ER 4118HV-CF100). Experiments were performed using a Bruker QT-II resonator and a pulsed Q-band Bruker E580 Elexsys spectrometer with an Applied Systems Engineering TWT amplifier (Model 177 Ka 300 W). The four pulse DEER sequence is as follows: $\pi_{obs}/2$- $\tau_1$-$\pi_{obs}$-($t$-$\pi_{pump}$)- ($\tau_2$-$t$)-$\pi_{obs}$- $\tau_2$-echo. Here, $\pi_{obs}$ is the observer pulse, $\pi_{pump}$ is the pump pulse, $t$ is the delay before the pump pulse, and $\tau_1$ and $\tau_2$ are pulse spacings. Nutation experiments were used to optimize observer pulse lengths (~10 ns for 90 pulses and ~20 ns for 180 pulses). The linear 100 ns chirp $\pi_{pump}$ frequency width was set at 80 MHz. For all experiments, $\pi_{obs}$ was set 90 MHz above the center of the pump frequency range. A series of 8 $\tau_1$ values in 16 ns increments was used to suppress artifacts from electron spin echo envelope modulation. $\tau_2$ is set at 6 µs for all experiments. All DEER experiments were signal averaged over at least 20 averages. End-to-end distance distributions were extracted by "model-free" Tikhonov regularization as executed by the LongDistances software.[19]

**Two-tailed independent t-test.**

$$t = \frac{\overline{x_1} - \overline{x_2}}{s_p \sqrt{\frac{1}{n_1} + \frac{1}{n_2}}}, \text{ with } s_p = \sqrt{\frac{(n_1 - 1)s_1^2 + (n_2 - 1)s_2^2}{n_1 + n_2 - 2}}$$
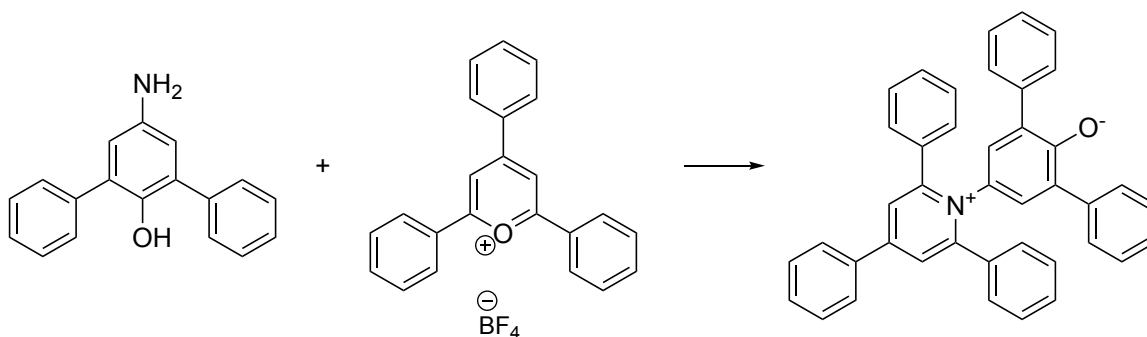
| Variable | Definition |
|---|---|
| $\overline{x_1}, \overline{x_2}$ | Mean of first and second sample |
| $n_1, n_2$ | Sample size of the first and samples |
| $s_1, s_2$ | Standard deviation of each sample |
| $s_p$ | Pooled variance |

Example:  Comparing $R_{max}$ of r1 and dib from atomistic simulations (Table S1).

Mean $R_{max}$ of r1 = 2.30, standard deviation of r1 = 0.27.

Mean $R_{max}$ of dib = 2.27, standard deviation of dib = 0.28.

$t(99,998) = 15.48$, $p < 0.00005$



**Reichardt's Dye (Betaine-30) Synthesis:** Synthetic procedure was adapted from existing literature.[20] To a 50-mL two-necked round-bottomed flask containing 0.172 g (0.658 mmol) 4-amine-2,6-diphenylphenol, 0.245 g (0.618 mmol) 2,4,6-triphenylpyrylium tetrafluoroborate, and 0.245 g (2.99 mmol) anhydrous sodium acetate, 3.1 mL (53.1 mmol) of ethanol was added. Then, the flask was placed in an oil bath and the reaction was refluxed at 92°C for four hours while stirring. The reaction was cooled to ambient temperature and stirred overnight. The product was precipitated by adding the resulting mixture dropwise to 100 mL 10% NaOH and stirring for three hours. This yielded dark blue crystals indicative of the hydrated product, which were isolated via vacuum filtration through a nylon filter. Transfer from the filter to a vial was facilitated by rinsing it with a small amount of ethanol. This vial was then lyophilized to give 333.6 mg (0.605 mmol) anhydrous green product with 95% purity for a 98% yield. ^{1}H NMR (600 MHz, MeOD) δ = 8.45 (dd, J = 1.6 Hz, 2H), 8.16 – 8.10 (m, 2H), 7.68 – 7.61 (m, 3H), 7.58 – 7.51 (m, 4H), 7.47 (dd, J = 5.0, 1.9 Hz, 6H), 7.25 – 7.19 (m, 8H), 7.15 (tt, J = 6.4, 1.8 Hz, 2H), 6.84 (d, J = 3.7 Hz, 2H). **Figure S16.**

**Incubating Peptoids On-Bead with Reichardt's Dye:** Reichardt's dye was dissolved in 10 mM DMSO solution. The dye was then diluted to 0.150 mM in buffer (HEPES, 100 mM, pH = 7.8). The solution was stirred overnight, and then was centrifuged down to pellet any suspended material. The supernatant of the dye and buffer solution was used for subsequent immobilized assays. PEGA resin with immobilized peptoid (1 mg) added in falcon tube with 5 mL of the dye and buffer supernatant solution. Samples were stirred at 37 ºC for 48 h before being imaged on Olympus MVX10 brightfield microscope.
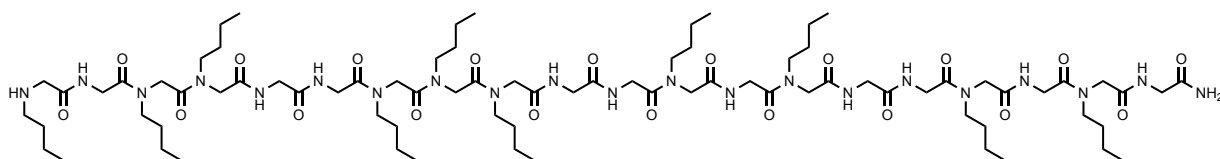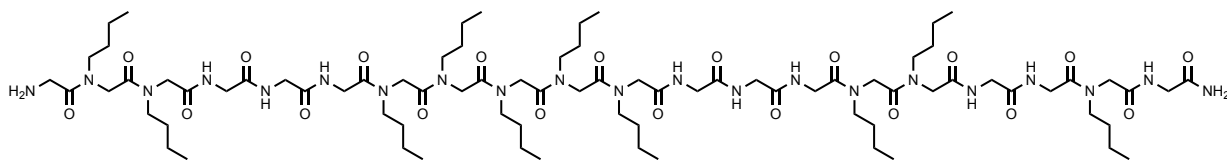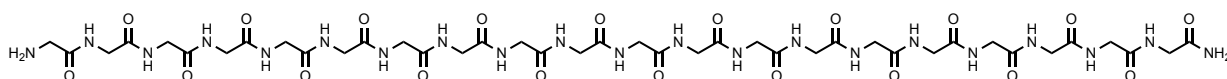
**Supplemental Figures:**
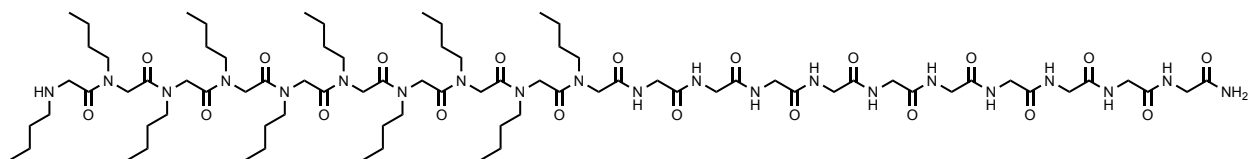


**diblock**
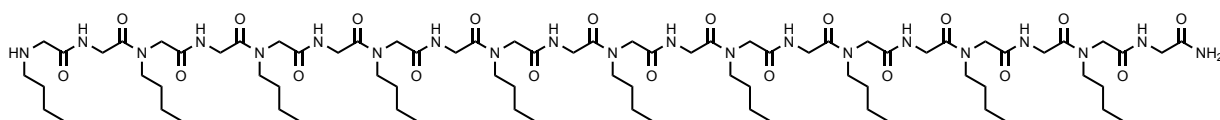


**alternating**



**randomized-1**



**randomized-2**



**homoglycine 20mer**

**Figure S1.** Chemical structure of the five peptidomimetic 20mers studied herein: diblock (**dib**), alternating (**alt**), randomized-1 (**r1**), randomized-2 (**r2**), and homoglycine 20mer (**gly$_{20}$**).
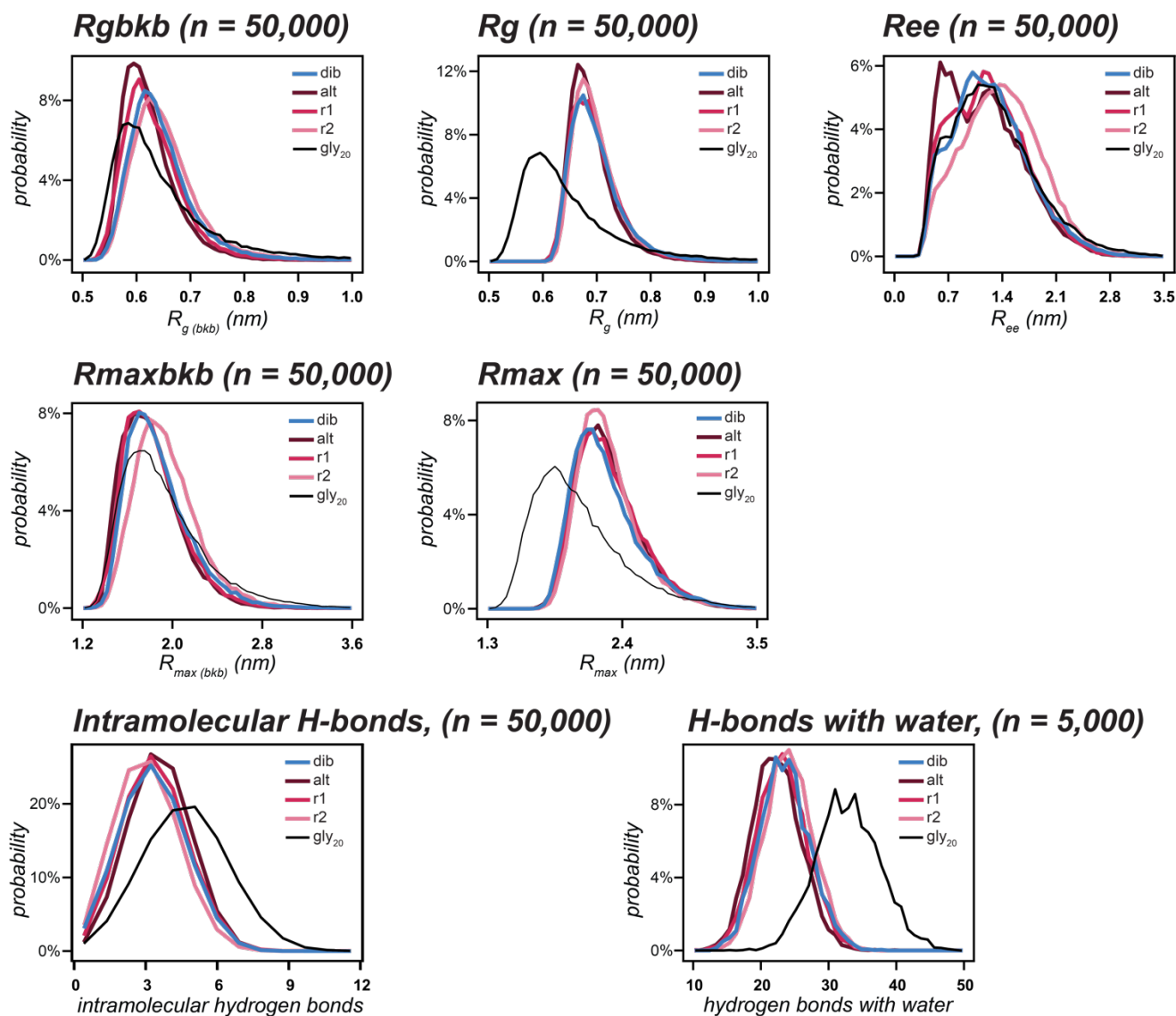
**Figure S2. Distribution of measurements from atomistic modeling.** Distribution plots for all previous described measurements for the five peptidomimetic macromolecules. $R_g$ and $R_{max}$ plots (middle) indicate the measurements obtained considering all atoms from peptoids, while $R_{g(bkb)}$ and $R_{max(bkb)}$ plots (left) were obtained from the backbone atoms.

**Table S1: Size measurements from atomistic modeling.** Average, standard deviation, and median of 50,000 conformations of each structure. Measurements include radius of gyration of the full macromolecule ($R_g$) and backbone mass only, excluding sidechain contributions ($R_{g\,(bkb)}$); maximum end-to-end distance of the full macromolecule ($R_{max}$) and backbone only ($R_{max\,(bkb)}$); and end-to-end distance of the macromolecule.

| Measurement | Sequence | Average (nm) | std dev (nm) | Median (nm) |
|---|---|---|---|---|
| | alt | 0.623 | 0.048 | 0.614 |
| | r1 | 0.631 | 0.054 | 0.622 |
| Rg (bkb) | r2 | 0.652 | 0.061 | 0.642 |
| | dib | 0.645 | 0.060 | 0.634 |
| | glycine 20mer | 0.645 | 0.095 | 0.620 |
| | alt | 1.81 | 0.25 | 1.77 |
| | r1 | 1.83 | 0.26 | 1.79 |
| Rmax (bkb) | r2 | 1.95 | 0.28 | 1.91 |
| | dib | 1.88 | 0.28 | 1.82 |
| | glycine 20mer | 1.92 | 0.37 | 1.85 |
| | alt | 1.16 | 0.49 | 1.13 |
| | r1 | 1.23 | 0.48 | 1.20 |
| Ree | r2 | 1.39 | 0.49 | 1.38 |
| | dib | 1.25 | 0.49 | 1.21 |
| | glycine 20mer | 1.29 | 0.54 | 1.23 |
| | alt | 0.690 | 0.041 | 0.682 |
| | r1 | 0.697 | 0.047 | 0.688 |
| Rg | r2 | 0.700 | 0.049 | 0.690 |
| | dib | 0.699 | 0.051 | 0.689 |
| | glycine 20mer | 0.649 | 0.095 | 0.624 |
| | alt | 2.28 | 0.25 | 2.24 |
| | r1 | 2.30 | 0.27 | 2.25 |
| Rmax | r2 | 2.28 | 0.25 | 2.25 |
| | dib | 2.27 | 0.28 | 2.22 |
| | glycine 20mer | 2.04 | 0.37 | 1.97 |

**Table S2. Conformations from atomistic modeling clustered based on self-similarity.** For each sequence, 50,000 conformations were grouped based on 1.0 Å and 1.4 Å thresholds for similar conformations.

| | Sequence | number of clusters | % of population in top cluster |
|---|---|---|---|
| 1.0 Å cutoff` | alt | 14902 | 3.02% |
| | r1 | 17284 | 0.91% |
| | r2 | 22182 | 0.33% |
| | dib | 27583 | 0.75% |
| 1.4 Å cutoff | alt | 6954 | 3.54% |
| | r1 | 8275 | 1.03% |
| | r2 | 10813 | 0.49% |
| | dib | 14385 | 1.13% |

**Table S3. Comparison of clustering methods.** The simulated peptoids were clustered using three calculation methods. Each ordered pair in the table below indicates first the number of frames in the most abundant cluster, followed by the total number of clusters.

| | GROMOS | Linkage | Jarvis-Patrick |
|---|---|---|---|
| alt | 134; 3694 | 179; 3602 | 139; 4418 |
| r1 | 32; 3914 | 35; 3827 | 34; 4495 |
| r2 | 19; 4379 | 29; 4336 | 14; 4853 |
| dib | 40; 4658 | 61; 4641 | 58; 4920 |

**Table S4. Hydrogen bonds from atomistic modeling.** Average, standard deviation, and median of intramolecular hydrogen bonds (n = 50,000 conformations) and hydrogen bonds with water (n = 5,000 conformations) for each sequence.

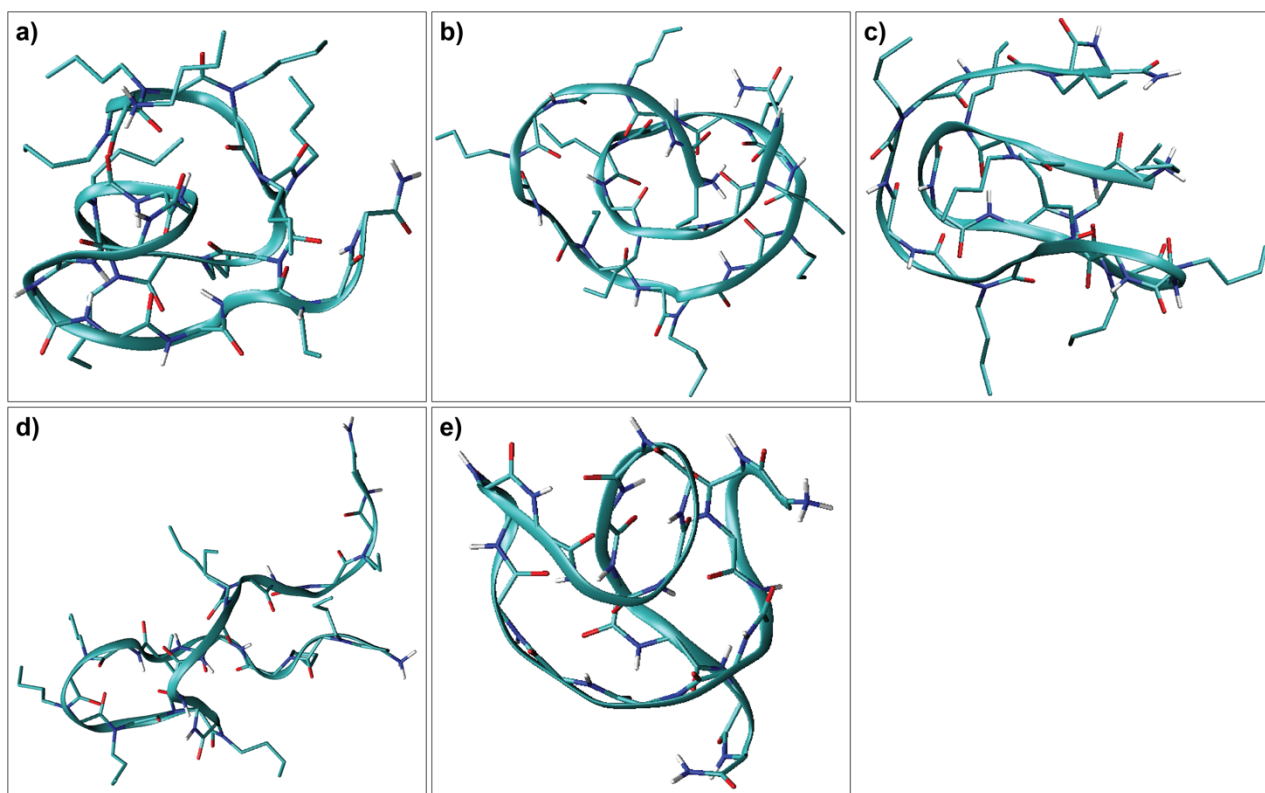| Measurement | Sequence | Average | std dev | Median |
|---|---|---|---|---|
| H-bonds, intramolecular | alt | 3.40 | 1.42 | 3 |
| | r1 | 3.19 | 1.47 | 3 |
| | r2 | 2.83 | 1.44 | 3 |
| | dib | 3.10 | 1.50 | 3 |
| | glycine 20mer | 4.59 | 1.95 | 5 |
| H-bonds, water | alt | 22.2 | 3.7 | 22 |
| | r1 | 23.0 | 3.8 | 23 |
| | r2 | 24.0 | 3.7 | 24 |
| | dib | 23.4 | 3.8 | 23 |
| | glycine 20mer | 33.0 | 4.8 | 33 |

**Figure S3.** Representations of simulated peptoids of highest abundance conformations from clustering (1.4 Å cut-off) for a) **dib**, b) **alt**, c) **r1**, d) **r2**, and e) **gly$_{20}$**.
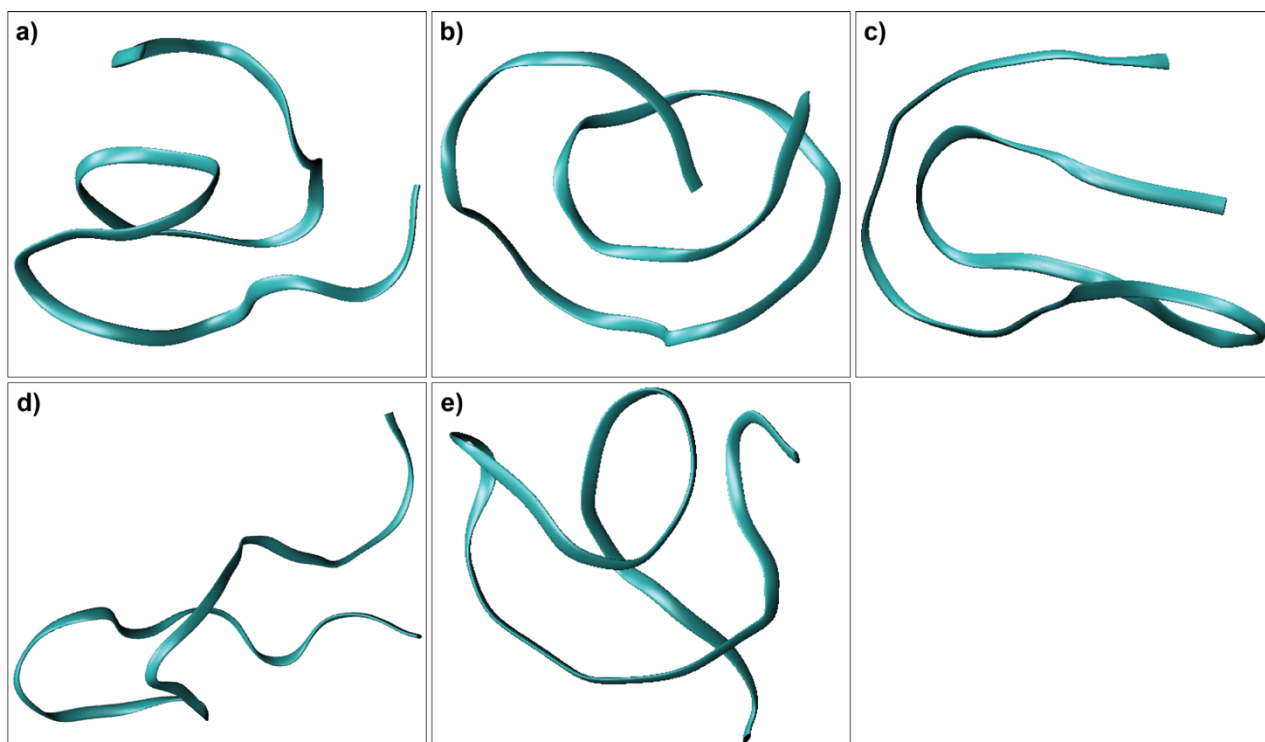


**Figure S4.** Representations of simulated peptoids excluding side-chains (backbone only) of highest abundance conformations from clustering (1.4 Å cut-off) for a) **dib**, b) **alt**, c) **r1**, d) **r2**, and e) **gly$_{20}$**.
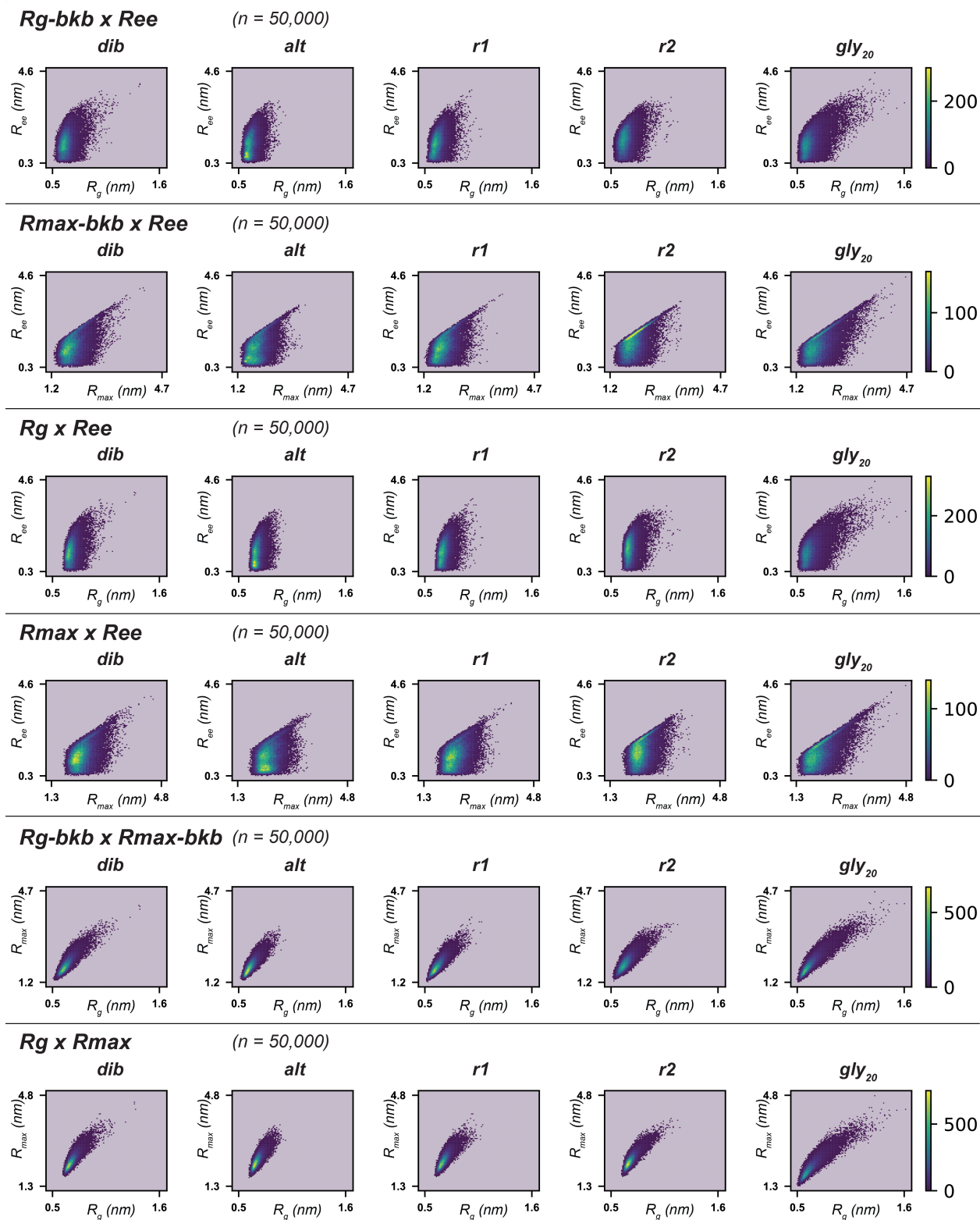
**Rg-bkb x Ree**   *(n = 50,000)*



**Rmax-bkb x Ree**   *(n = 50,000)*



**Rg x Ree**   *(n = 50,000)*



**Rmax x Ree**   *(n = 50,000)*



**Rg-bkb x Rmax-bkb**   *(n = 50,000)*



**Rg x Rmax**   *(n = 50,000)*



**Figure S5. Comparing measurements from atomistic simulations.** 2D distribution plots comparing metrics of 50,000 simulated conformations for each of the peptidomimetics. $R_g$ and $R_{max}$ plots indicate the measurements obtained considering all atoms from peptoids, while $R_{g(bkb)}$ and $R_{max(bkb)}$ plots on were obtained from the backbone atoms.
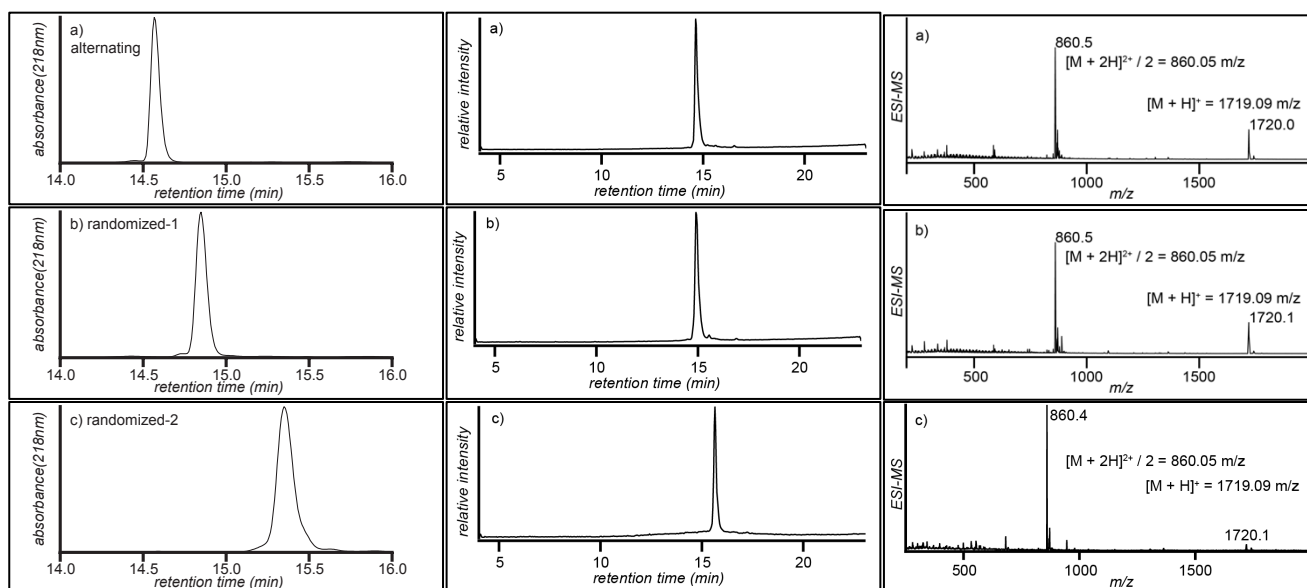
**Figure S6. LC-MS of purified peptoids.** LC-traces were run on a Phenomenex Aeris Peptide C18 column (100 × 4.6 mm) and monitored at 218 nm (left). Mass chromatogram (center) of positive mode (600-2000 m/z). ESI mass spectrum (right) was obtained by integrating over the entire retention time. Spectra shown for purified 20mers a) **alt** peptoid, b) **r1** peptoid, c) **r2** peptoid.
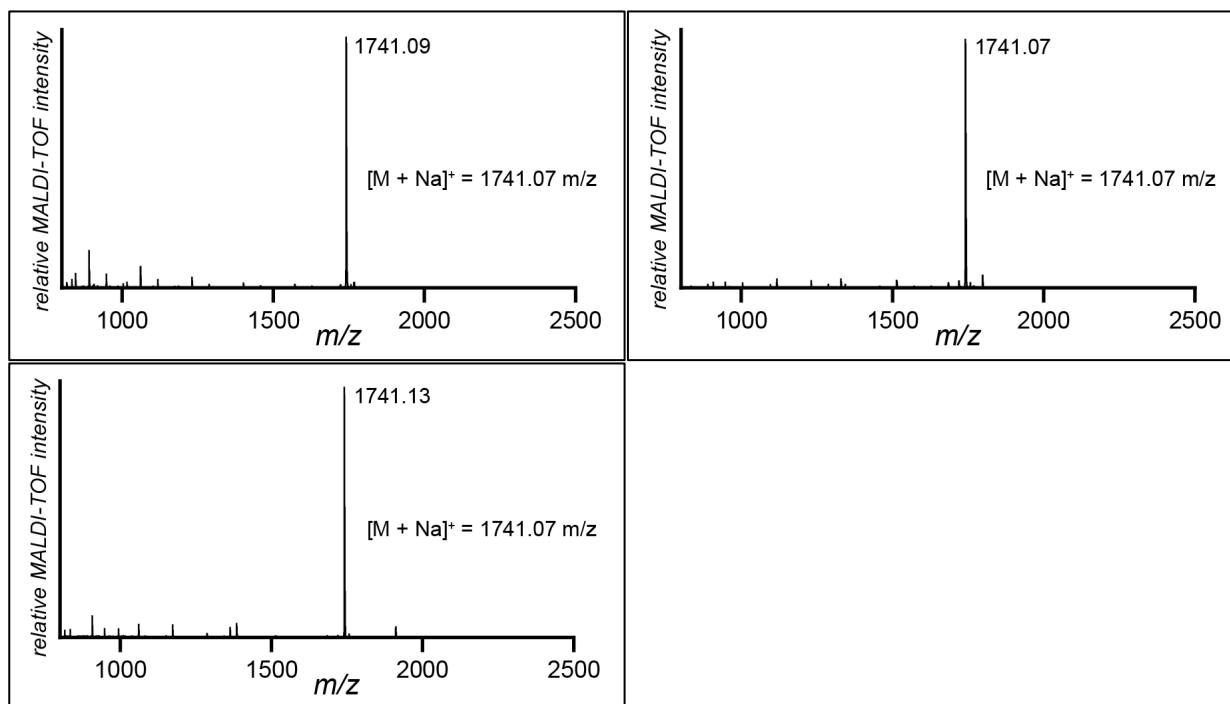


**Figure S7. MALDI-TOF of purified peptoids.** Sodium adducts of peptoids observed in positive mode ionization. Spectra shown for a) **alt** peptoid, b) **r1** peptoid, c) **r2** peptoid.

**A)**  **Chromatography Parameters**

**Column:** Raptor C18, 1.8 µm, 50 mm × 2.1 mm (cat.#. 9304252)
**Guard Column:** None
**Mobile Phase A:** 5 mM ammonium acetate in water
**Mobile Phase B:** 50/50 methanol/acetonitrile
**Column Temperature:** 60 °C

**B)**  **IMS-MS Parameters**

**Tuning and Mass Range:** 50-1700 *m/z*, High Sensitivity Mode

**Ionization Mode:** ESI (Agilent Jet Stream), Negative Polarity

**Source Settings:** Gas Temp, 325 °C; Drying Gas, 10 L/min; Nebulizer, 40 PSI; Sheath Gas Temp, 275 °C; Sheath Gas Flow, 12 L/min; Vcap, 4000 V; Nozzle Voltage, 2000 V; Fragmentor, 400 V

**IMS Settings:** Nitrogen Drift Gas, Pressurized at 3.95 Torr. Drift Tube Entrance Voltage, -1574 V; Drift Tube Exit Voltage, -224 V; Rear Funnel Entrance Voltage, -217.5 V; Rear Funnel Exit, -45 V

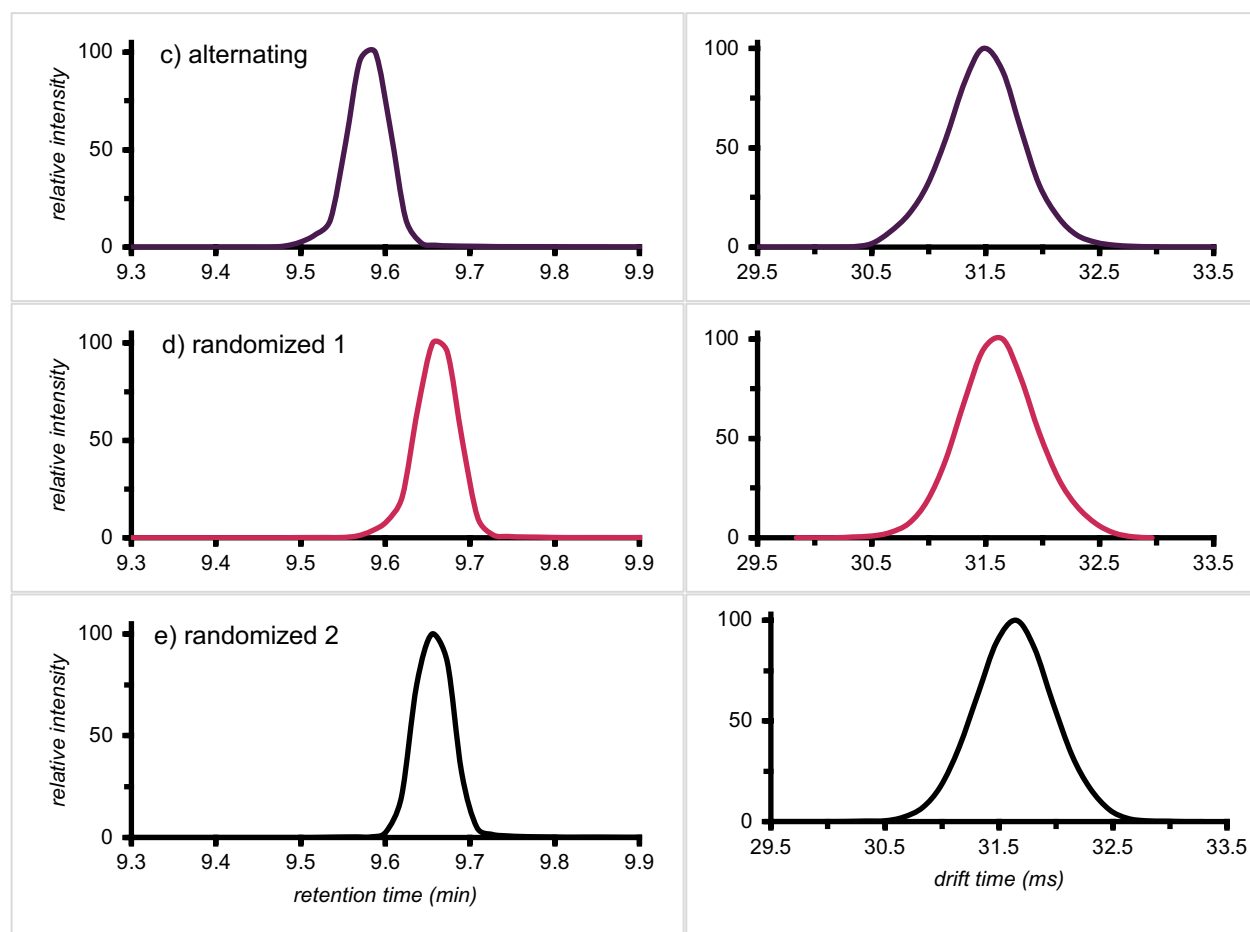| Time (min) | Flow Rate (mL/min) | %B |
|---|---|---|
| 0 | 0.5 | 15 |
| 2 | 0.5 | 15 |
| 4 | 0.5 | 35 |
| 6 | 0.5 | 40 |
| 7.5 | 0.5 | 50 |
| 8.6 | 0.5 | 55 |
| 9.7 | 0.8 | 80 |
| 9.9 | 0.8 | 85 |
| 10.5 | 0.8 | 85 |
| 10.51 | 0.5 | 15 |
| 12.5 | 0.5 | 15 |



**Figure S8. LC-IMS-MS acquisition settings and representative chromatograms. a)** Extended chromatographic settings used for peptoid separations prior to IMS-MS analysis performed on the Agilent 6560 IM-MS featuring extended settings noted in **b**. Representative LC-IMS-MS chromatograms, including LC-MS traces (left) of purified peptoid samples and IMS chromatograms (right) of doubly protonated charge state (z = +2) of for c) **alt** peptoid, d) **r1** peptoid, and e) **r2** peptoid.
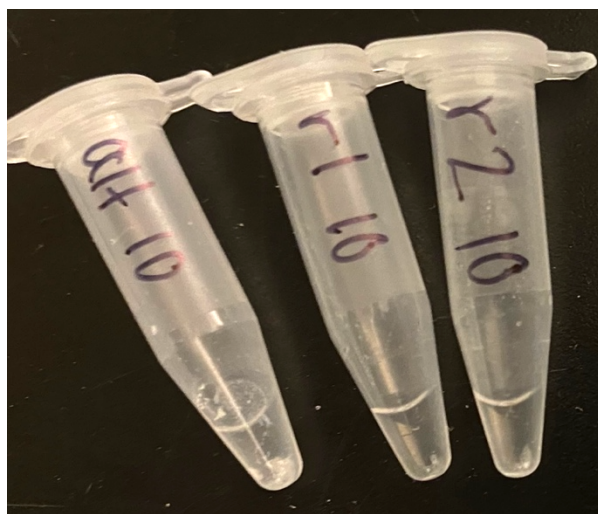
**Figure S9**. **Visually apparently aggregation.** Image of peptoids **alt**, **r1**, and **r2** prepared at 10 mg/mL in 100 mM HEPES pH 7.8 captured with an iPhone 11 Pro. **Alt** visibly has undissolved material, whereas **r1** and **r2** are fully dissolved.
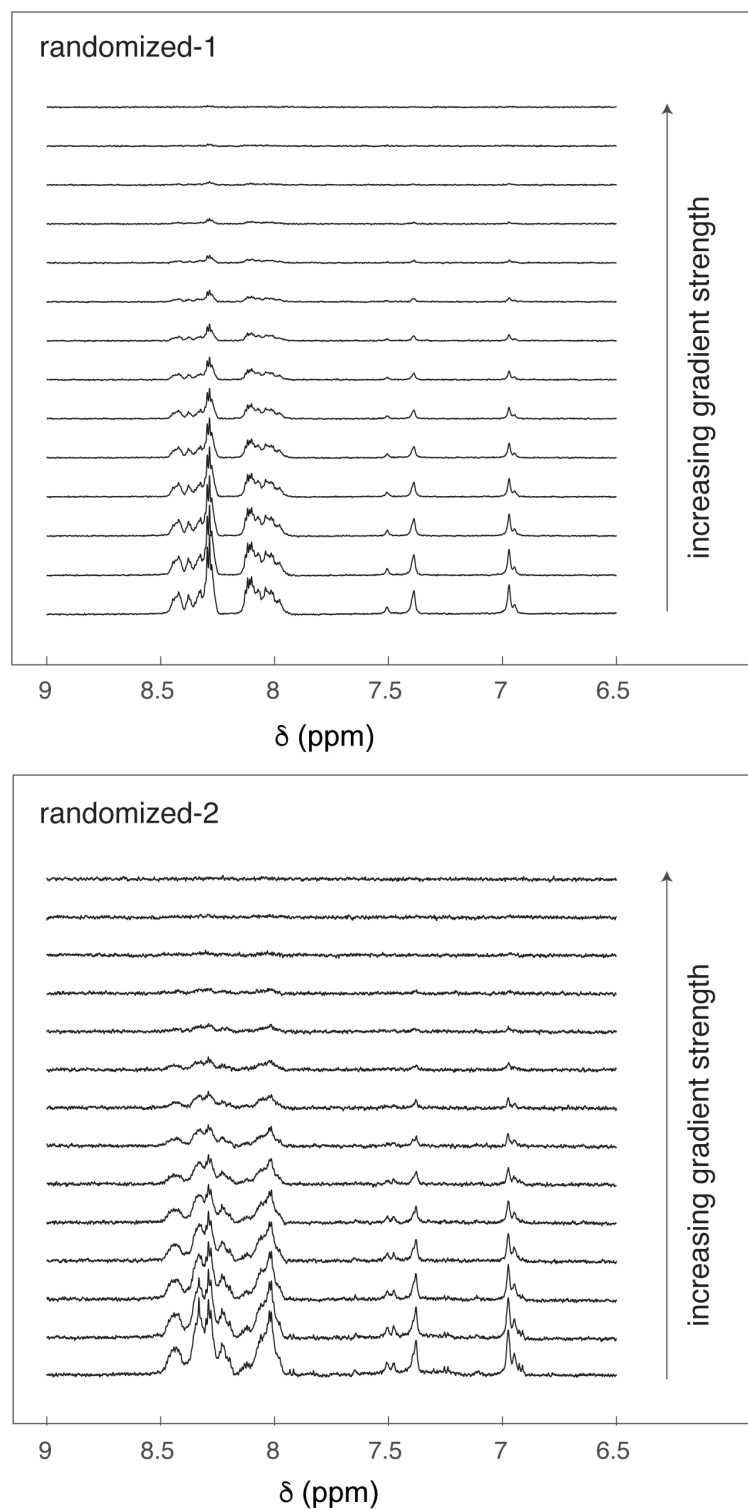
**Figure S10. DOSY spectra.** Arrayed NMR spectra from DOSY measurements for peptoids **r1** (top) and **r2** (bottom).

Diffusion constants were $3.3 \pm 0.1$ and $3.4 \pm 0.2 \times 10^{-10}$ m$^2$ s$^{-1}$ for **r1** and **r2**, respectively. A two-tailed t-test comparing the diffusion constants revealed that the samples exhibited statistically insignificant differences, with a confidence level of 50% (t(2) = 0.85, $p < 0.5$).
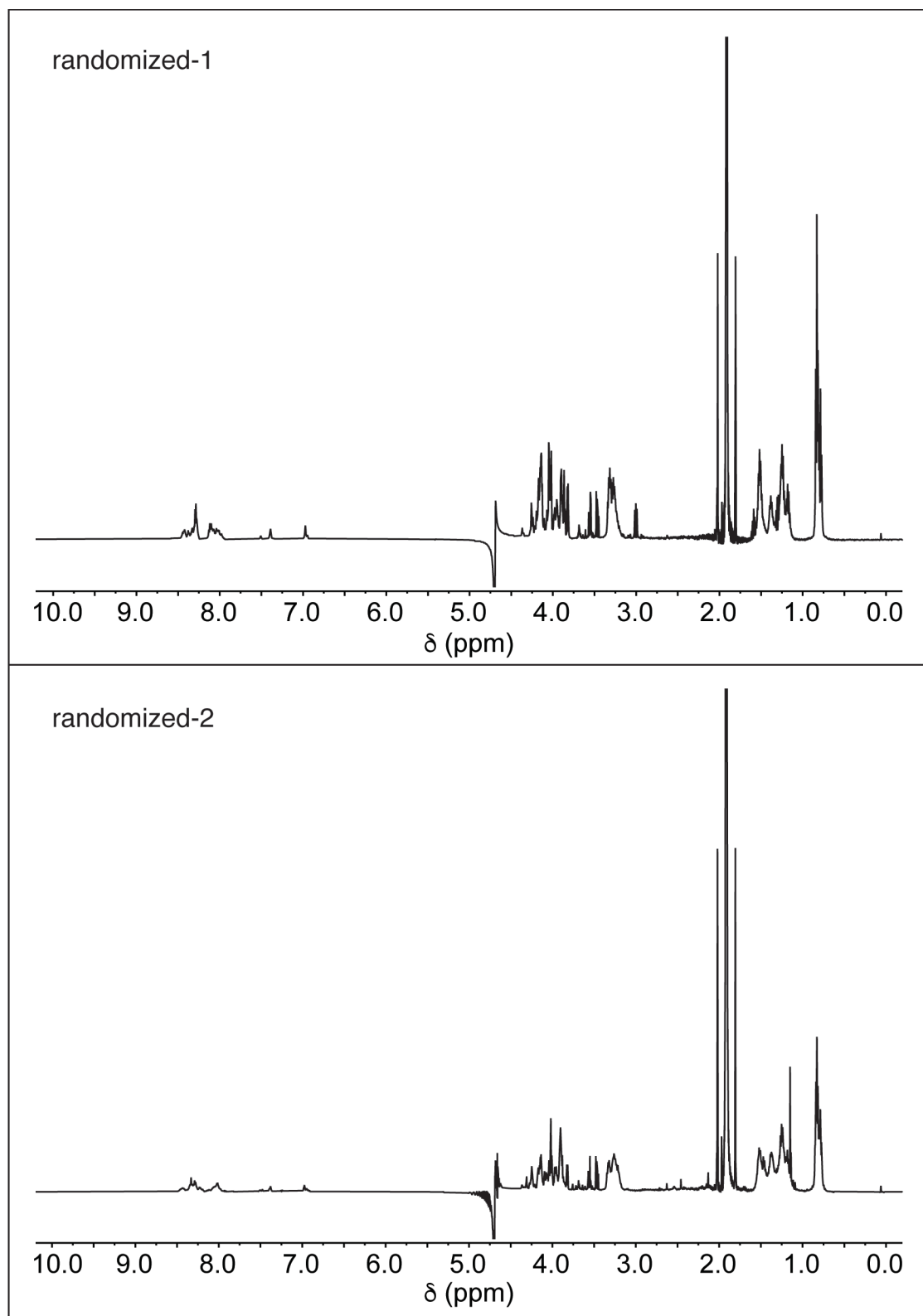
**Figure S11. ^{1}H- NMR Spectra.** Full ^{1}H- NMR spectra of peptoids **r1** (top) and **r2** (bottom) in 50 mM sodium acetate buffer (pH 4.5).
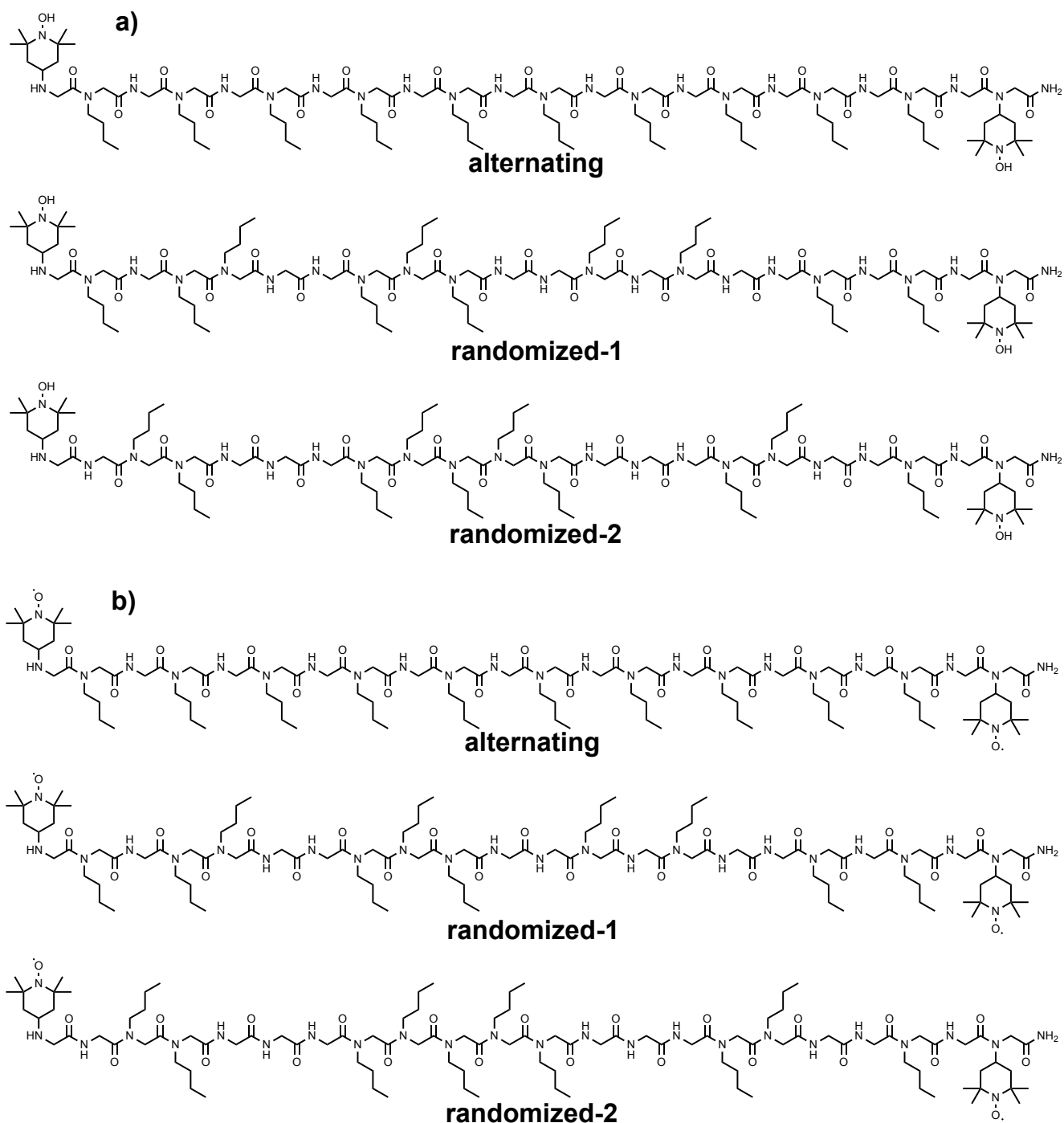
**Figure S12. Chemical structures of the TEMPO peptoids.** Three peptoid sequences, alternating (**alt**), randomized-1 (**r1**), and randomized-2 (**r2**), with TEMPO residues. a) Structures of peptoids after cleaving from the resin with trifluoroacetic acid (TFA) and characterized in **Figures S13-14**. b) Peptoids used for DEER spectroscopy after reintroduction of the radicals with ammonia.
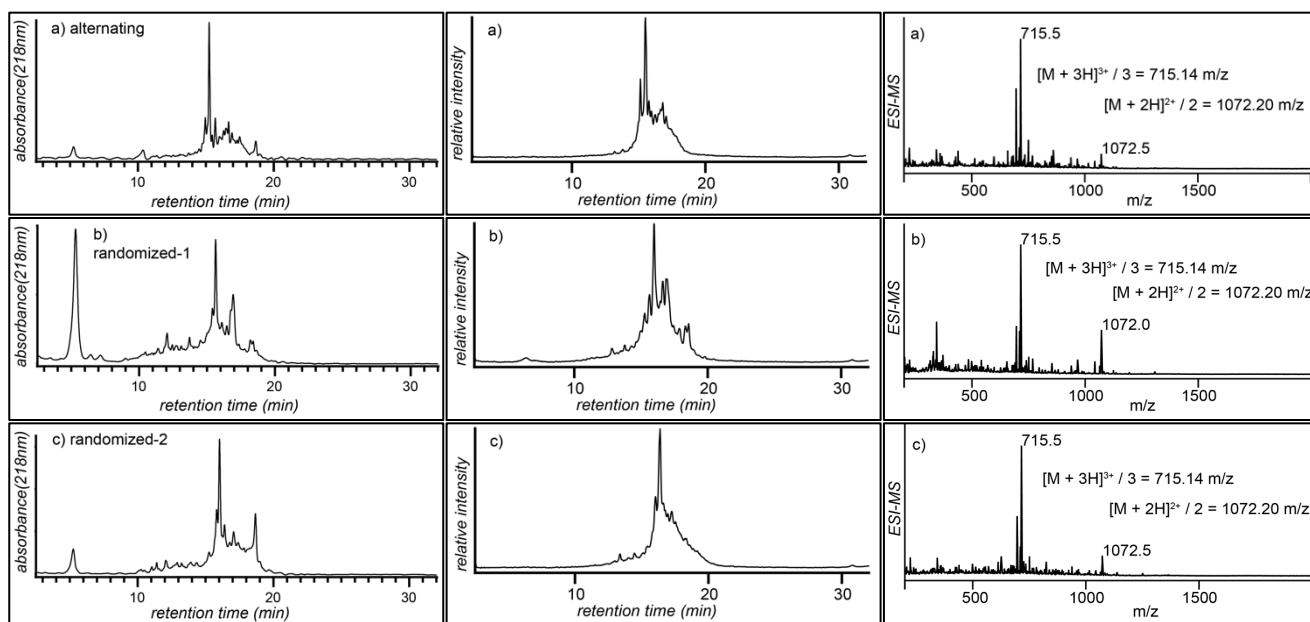
**Figure S13. LC-MS of unpurified peptoids with two TEMPO monomers.** LC-traces (left) were run on a Shimadzu Nexcol C18 5 μm (50 × 3.0 mm) and monitored at 218 nm. Mass chromatogram (center) of positive mode (600-2000 m/z). ESI mass spectrum (right) was obtained by integrating over the entire retention time. Spectra shown for a) **alt** peptoid, b) **r1** peptoid, and c) **r2** peptoid.
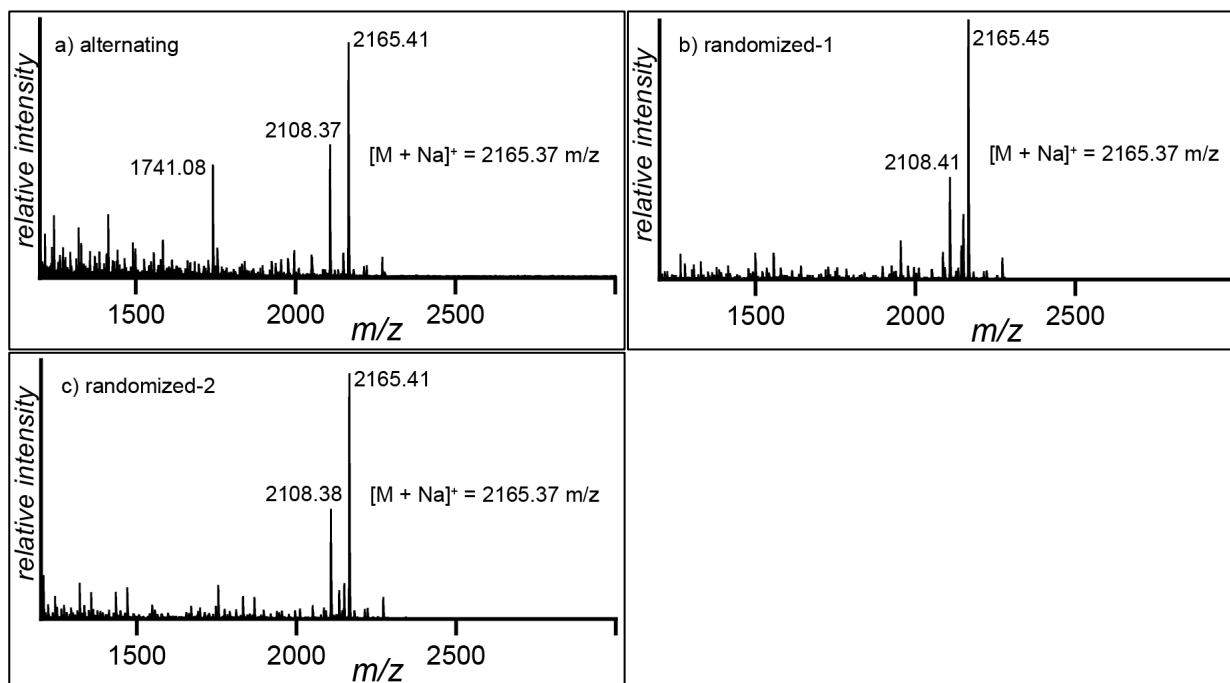


**Figure S14. MALDI-TOF of peptoids with two TEMPO monomers.** Sodium adducts of peptoids observed in positive mode ionization. Spectra shown for a) **alt** peptoid, b) **r1** peptoid, c) **r2** peptoid.
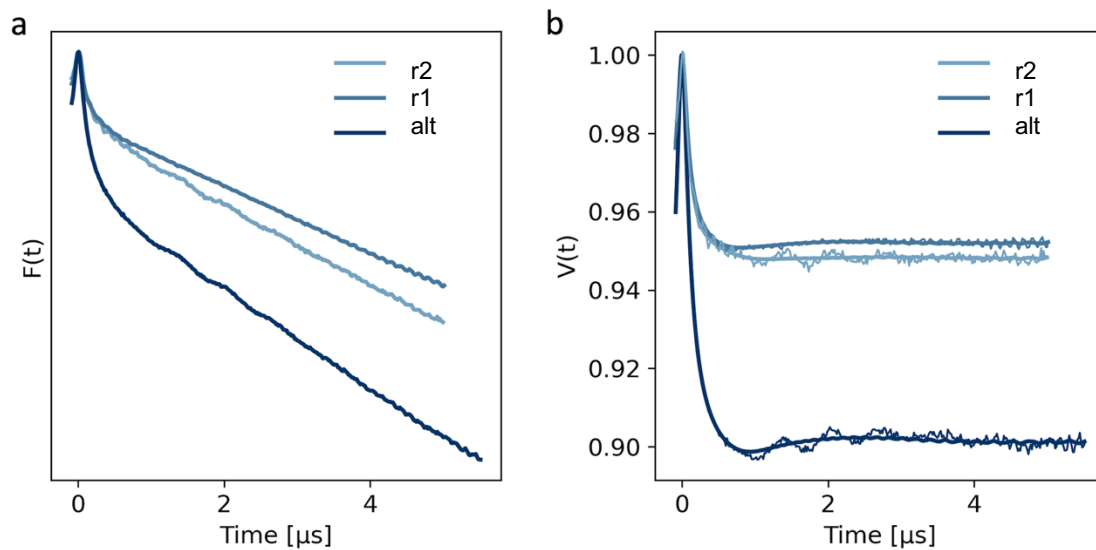
**Figure S15. Time-domain DEER spectra.** (a) Raw time domain spectra are (b) background corrected and fit (smooth lines) using model free Tikhonov regularization.
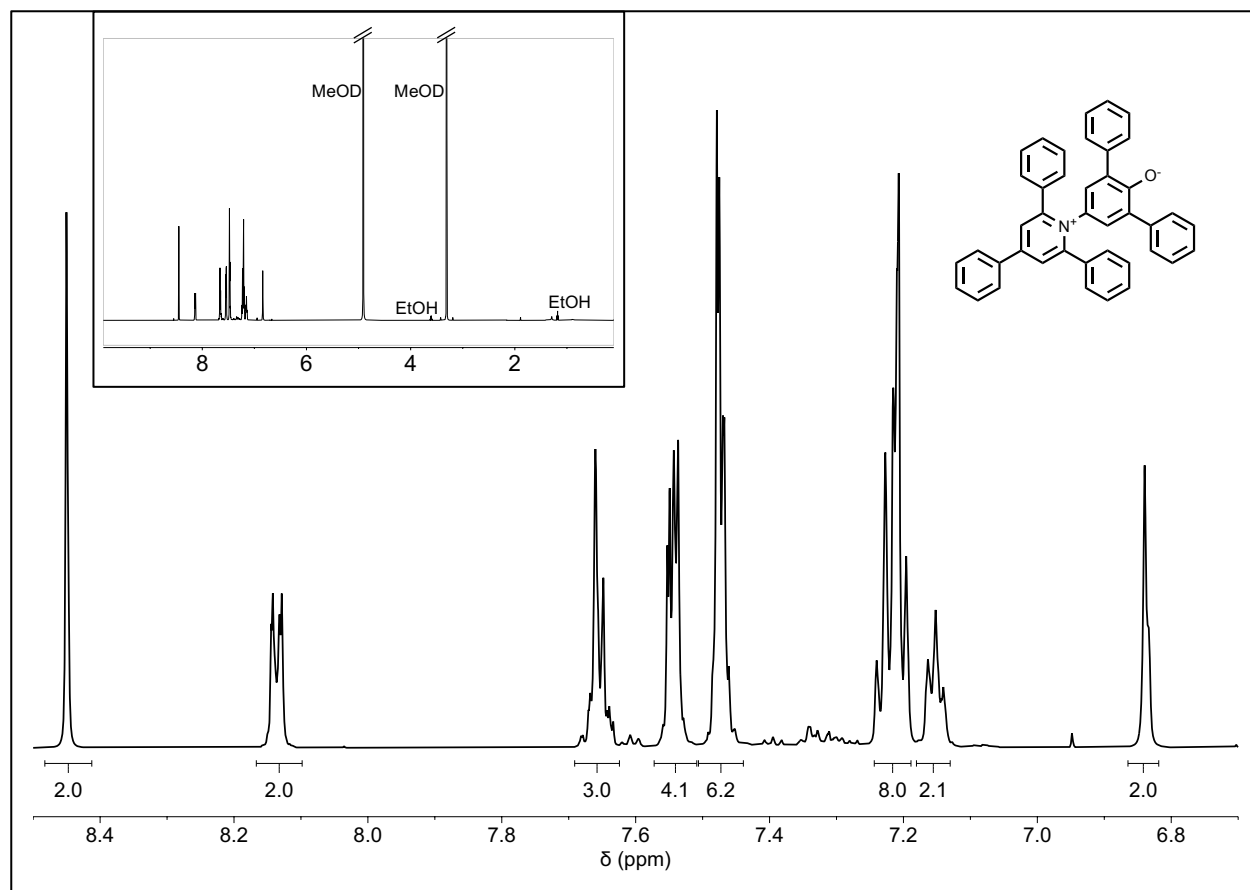
**Figure S16. Reichardt's dye ¹H NMR** (600 MHz, MeOD) δ = 8.45 (dd, J = 1.6 Hz, 2H), 8.16 – 8.10 (m, 2H), 7.68 – 7.61 (m, 3H), 7.58 – 7.51 (m, 4H), 7.47 (dd, J = 5.0, 1.9 Hz, 6H), 7.25 – 7.19 (m, 8H), 7.15 (tt, J = 6.4, 1.8 Hz, 2H), 6.84 (d, J = 3.7 Hz, 2H).
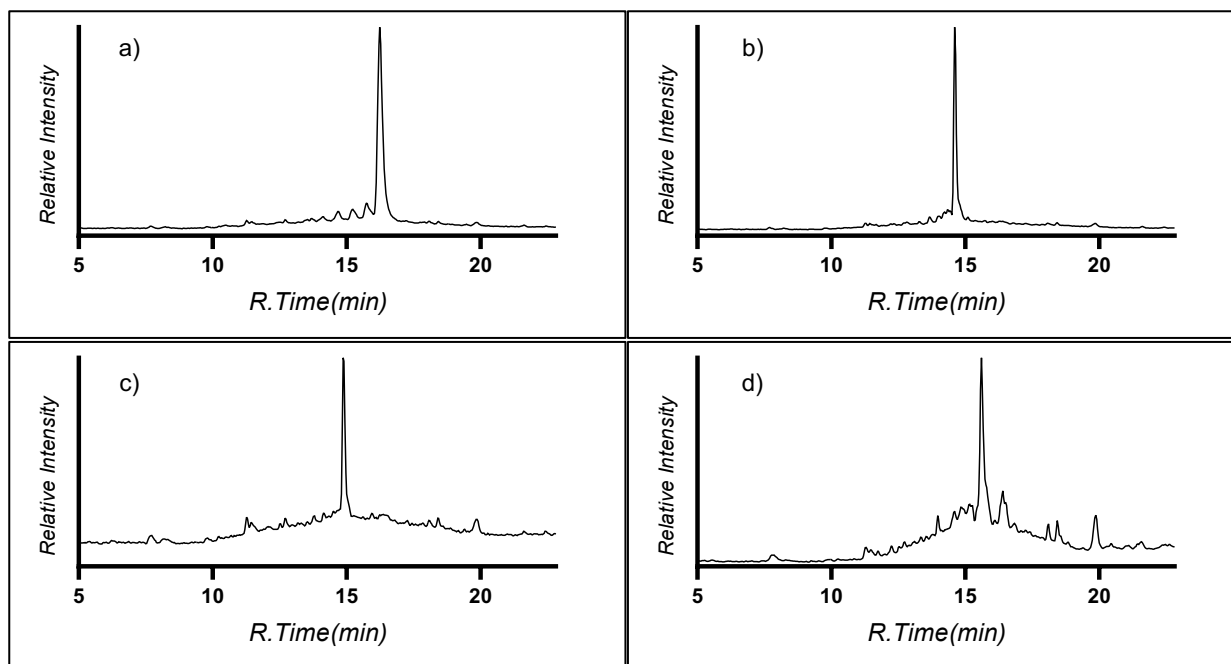
**Figure S17. LC-MS traces of PEGA samples.** Positive mode MS chromatogram (600-2000 m/z) ran on a Phenomenex Aeris Peptide C18 column (100 × 4.6 mm) of a) diblock 20mer, b) alternating 20mer, c) randomized-1 20mer (r1), d) randomized-2 20mer (r2), 20mer synthesized on rink amide PEGA resin.
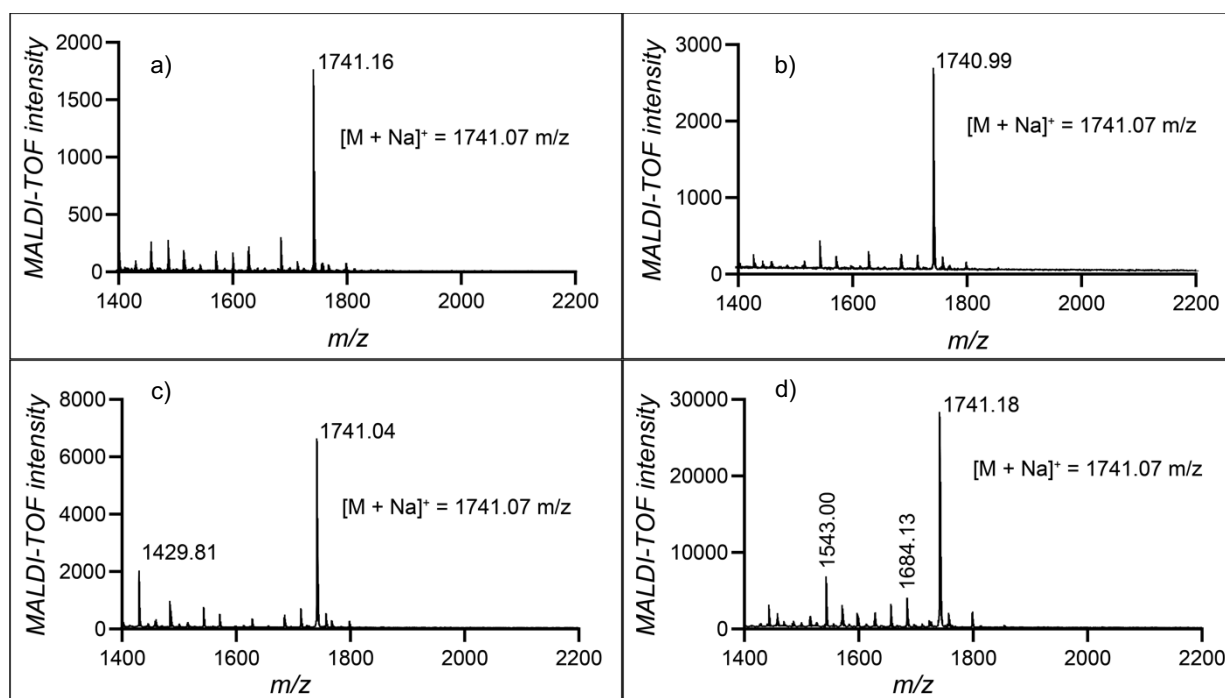


**Figure S18. MALDI-TOF of peptoids synthesized on PEGA resin.** Sodium adducts of peptoids observed in positive mode ionization. Spectra shown for a) **dib** peptoid b) **alt** peptoid, c) **r1** peptoid, and d) **r2** peptoid.
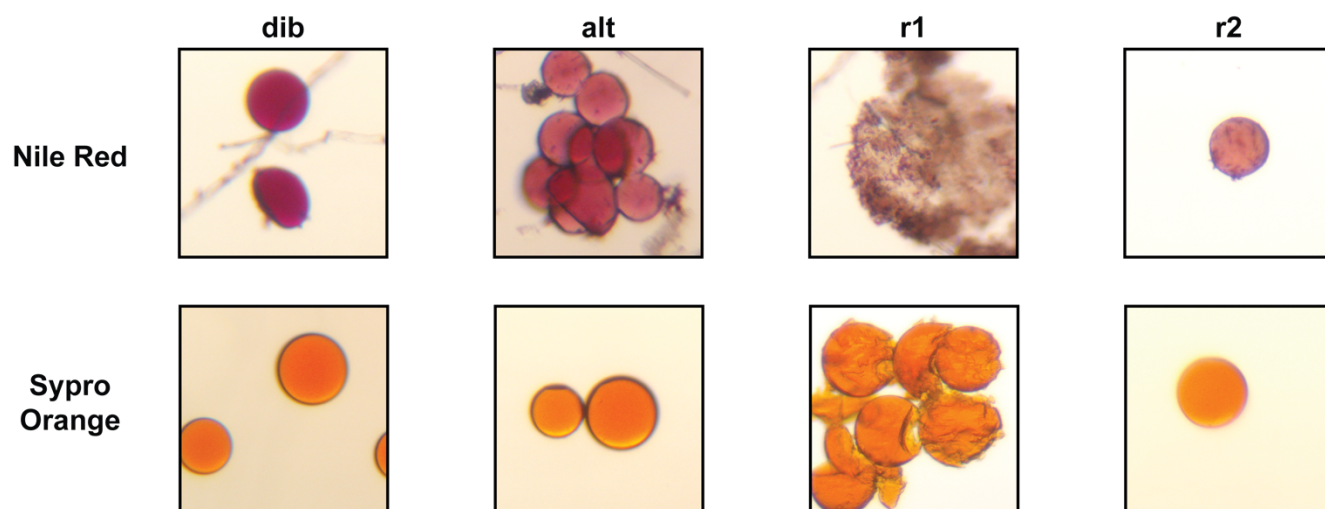
**Figure S19. Brightfield images of immobilized peptoids with Nile Red and Sypro Orange**. Each of the model peptoids were incubated at 37ºC for 48 hours in HEPES (100 mM, pH 7.8) with 150 µM Nile Red or 5X Sypro orange. Samples were imaged Olympus CK30 with 4X objective, 6V 30W Lamphouse and AMScope 1803 camera with eyepiece attachment.
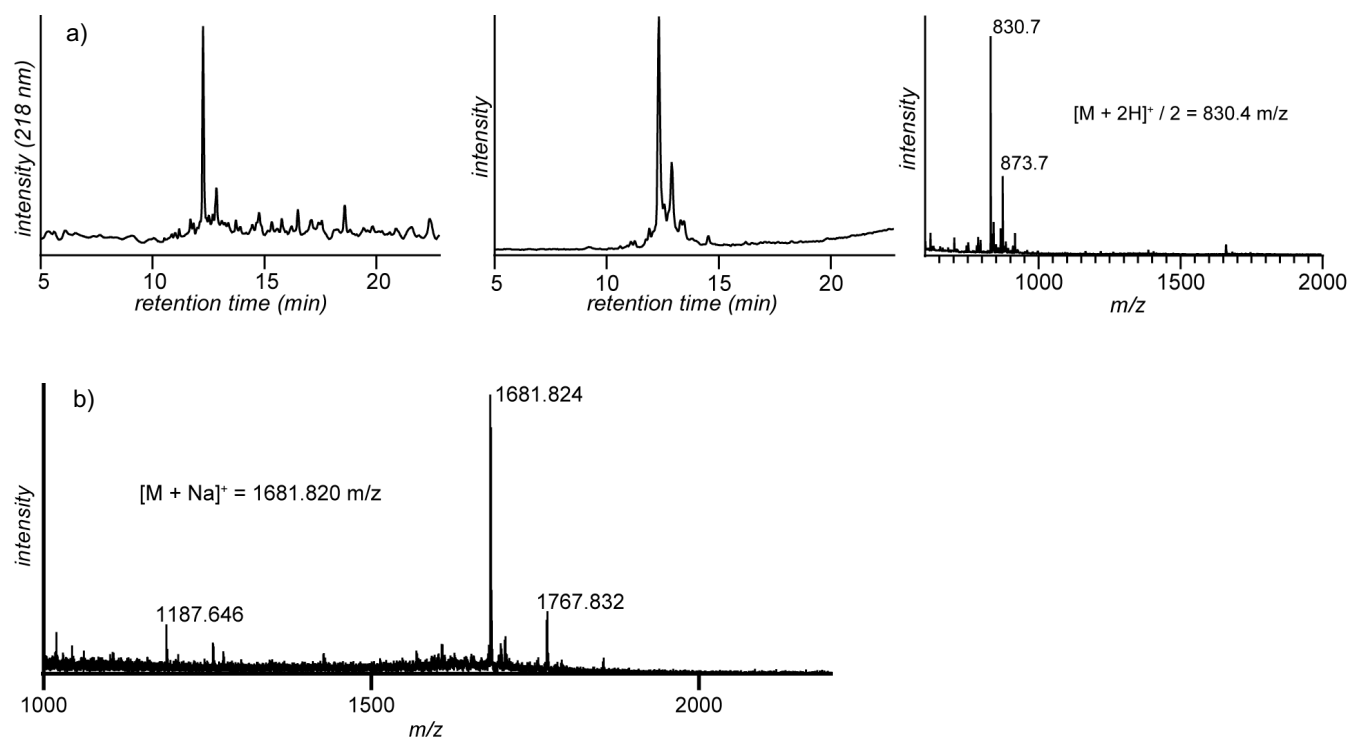
**Figure S20. Unstructured peptide characterization.** The PAS random coil peptide has sequence ASPAAPAPASASPAAPAPAS. a) LC-MS was run on a Phenomenex Aeris Peptide C18 column (100 × 4.6 mm) and monitored at 218 nm (left). Mass chromatogram (center) of positive mode (600-2000 m/z). ESI mass spectrum (right) was obtained by integrating over the entire retention time. b) MALDI spectra from positive mode ionization, annotated with the expected mass of the peptide.



**Figure S21. Unstructured peptide with Reichardt's dye.** Brightfield image PAS 20mer peptide on HMBA-PEGA resin, in presence of Reichardt's dye (0.150 mM in 100 mM HEPES pH 7.8).
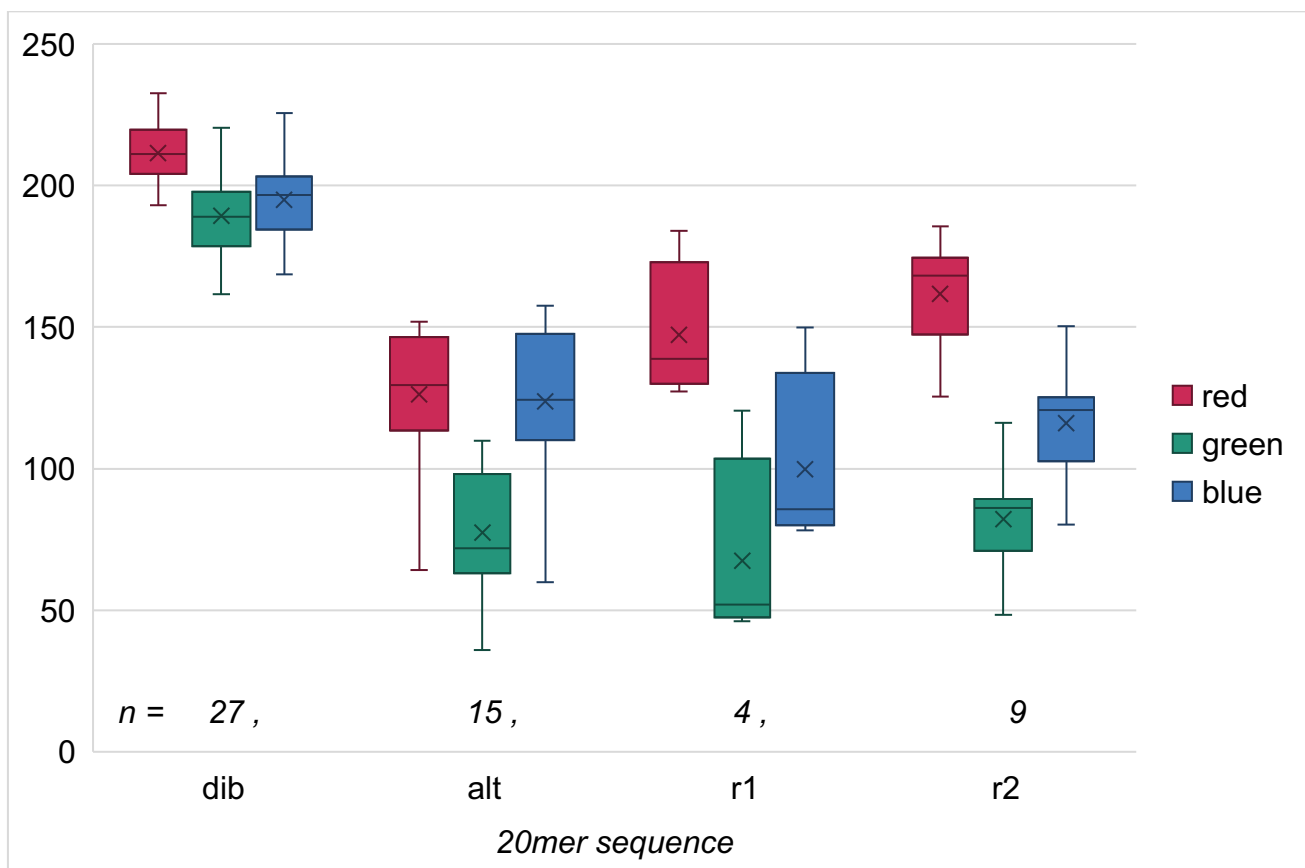
**Figure S22. Quantitation of RGB values of model sequences.** To quantify RGB, images were processed utilizing ImageJ software. Following conversion into an RGB stack, regions of interest (ROIs) were delineated encompassing each bead. Mean intensities for each color channel within these regions were extracted. Analysis was performed for full images from Figure S24 row 4.
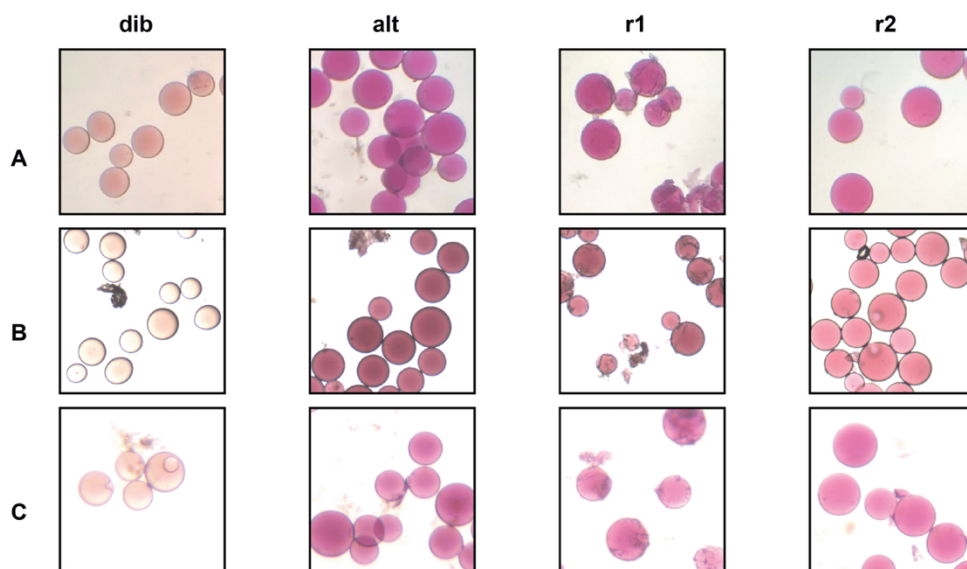
**Figure S23. Microscope comparison of dye stained peptoids on PEGA resin.** All images are from the same experiment and imaged on different systems. Images were taken on three different microscopes and digital camera pairs: (A) Bausch & Lomb upright microscope image with Apple iPhone 11 Pro, (B) Olympus IX81 Luna with QImaging RETIGA 4000R, and (C) Olympus CK30 with 4X objective, 6V 30W Lamphouse and AMScope 1803 camera with eyepiece attachment. (Note that iPhone images are the only rows with non-uniform white balance.)
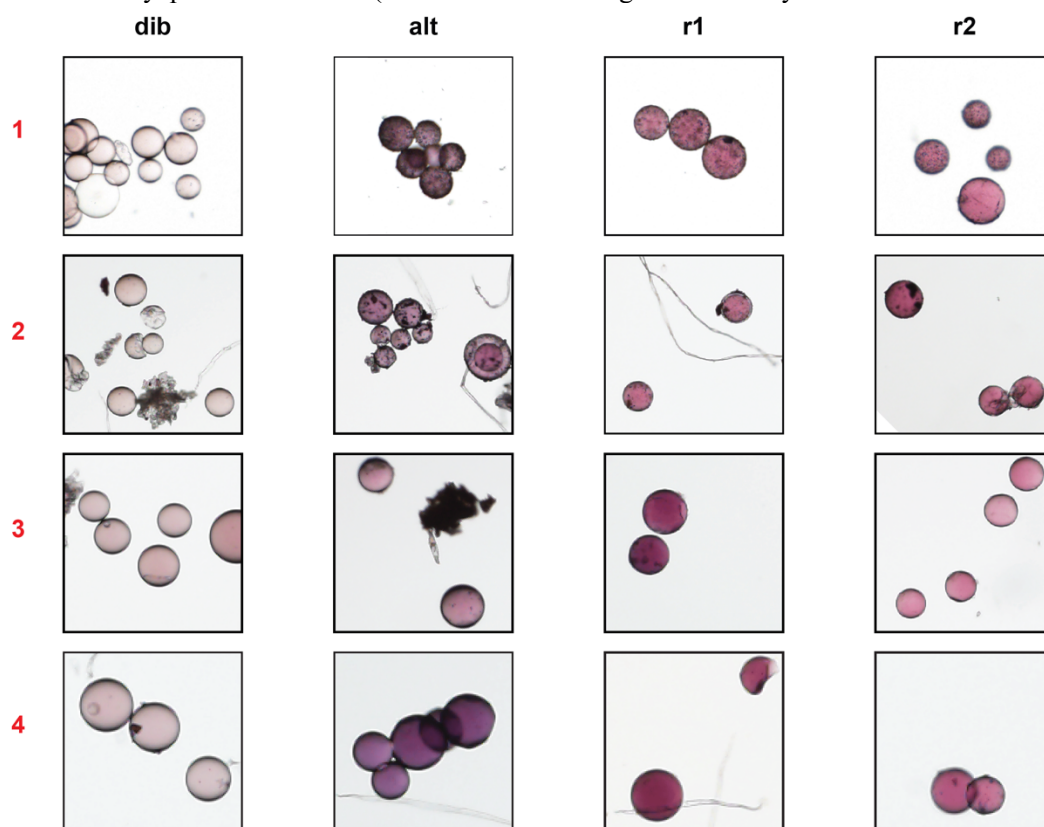


**Figure S24. Replicate incubating and imagine of peptoids on PEGA with Reichardt's dye.** Four preparations of peptoids on PEGA with Reichardt's dye assay, all imaged on an Olympus MVX10, upright stereoscope stand equipped with a 30W halogen lamp and with a MVPLAPO 1.0X objective and an Olympus DP80 Dual Sensor Color-Monochrome camera at 1.6 X, 8-bit, 4 × 4 μm.

**References**

(1) Simon, R. J.; Kania, R. S.; Zuckermann, R. N.; Huebner, V. D.; Jewell, D. A.; Banville, S.; Ng, S.; Wang, L.; Rosenberg, S.; Marlowe, C. K.; Spellmeyer, D. C.; Tan, R.; Frankel, A. D.; Santi, D. V.; Cohen, F. E.; Bartlett, P. A. Peptoids: A Modular Approach to Drug Discovery. *Proc. Natl. Acad. Sci. U. S. A.* **1992**, *89* (20), 9367–9371. https://doi.org/10.1073/pnas.89.20.9367.

(2) Zuckermann, R. N.; Kerr, J. M.; Moos, W. H.; Kent, S. B. H. Efficient Method for the Preparation of Peptoids [Oligo(N-Substituted Glycines)] by Submonomer Solid-Phase Synthesis. *J. Am. Chem. Soc.* **1992**, *114* (26), 10646–10647. https://doi.org/10.1021/ja00052a076.

(3) Van Der Spoel, D.; Lindahl, E.; Hess, B.; Groenhof, G.; Mark, A. E.; Berendsen, H. J. C. GROMACS: Fast, Flexible, and Free. *J. Comput. Chem.* **2005**, *26* (16), 1701–1718. https://doi.org/10.1002/jcc.20291.

(4) Berendsen, H. J. C.; Postma, J. P. M.; Van Gunsteren, W. F.; Hermans, J. Interaction Models for Water in Relation to Protein Hydration. In *Intermolecular Forces*; Pullman, B., Ed.; The Jerusalem Symposia on Quantum Chemistry and Biochemistry; Springer Netherlands: Dordrecht, 1981; Vol. 14, pp 331–342. https://doi.org/10.1007/978-94-015-7658-1_21.

(5) Hoover, W. G. Canonical Dynamics: Equilibrium Phase-Space Distributions. *Phys. Rev. A* **1985**, *31* (3), 1695–1697. https://doi.org/10.1103/PhysRevA.31.1695.

(6) Hess, B.; Bekker, H.; Berendsen, H. J. C.; Fraaije, J. G. E. M. LINCS: A Linear Constraint Solver for Molecular Simulations. *J. Comput. Chem.* **1997**, *18* (12), 1463–1472. https://doi.org/10.1002/(SICI)1096-987X(199709)18:12<1463::AID-JCC4>3.0.CO;2-H.

(7) Darden, T.; York, D.; Pedersen, L. Particle Mesh Ewald: An $N \cdot \log(N)$ Method for Ewald Sums in Large Systems. *J. Chem. Phys.* **1993**, *98* (12), 10089–10092. https://doi.org/10.1063/1.464397.

(8) Páll, S.; Hess, B. A Flexible Algorithm for Calculating Pair Interactions on SIMD Architectures. *Comput. Phys. Commun.* **2013**, *184* (12), 2641–2650. https://doi.org/10.1016/j.cpc.2013.06.003.

(9) Berendsen, H. J. C.; Postma, J. P. M.; Van Gunsteren, W. F.; DiNola, A.; Haak, J. R. Molecular Dynamics with Coupling to an External Bath. *J. Chem. Phys.* **1984**, *81* (8), 3684–3690. https://doi.org/10.1063/1.448118.

(10) Hockney, R. W. *The Potential Calculation and Some Applications. In Methods in Computational Physics*, Alder, B., Fernbach, S., Rotenberg, M., Eds.; Academic Press: New York, 1970; Vol. 9.

(11) May, J. C.; Goodwin, C. R.; Lareau, N. M.; Leaptrot, K. L.; Morris, C. B.; Kurulugama, R. T.; Mordehai, A.; Klein, C.; Barry, W.; Darland, E.; Overney, G.; Imatani, K.; Stafford, G. C.; Fjeldsted, J. C.; McLean, J. A. Conformational Ordering of Biomolecules in the Gas Phase: Nitrogen Collision Cross Sections Measured on a Prototype High Resolution Drift Tube Ion Mobility-Mass Spectrometer. *Anal. Chem.* **2014**, *86* (4), 2107–2116. https://doi.org/10.1021/ac4038448.

(12) May, J. C.; Dodds, J. N.; Kurulugama, R. T.; Stafford, G. C.; Fjeldsted, J. C.; McLean, J. A. Broadscale Resolving Power Performance of a High Precision Uniform Field Ion Mobility-Mass Spectrometer. *The Analyst* **2015**, *140* (20), 6824–6833. https://doi.org/10.1039/C5AN00923E.

(13) Stow, S. M.; Causon, T. J.; Zheng, X.; Kurulugama, R. T.; Mairinger, T.; May, J. C.; Rennie, E. E.; Baker, E. S.; Smith, R. D.; McLean, J. A.; Hann, S.; Fjeldsted, J. C. An Interlaboratory Evaluation of Drift Tube Ion Mobility–Mass Spectrometry Collision Cross Section Measurements. *Anal. Chem.* **2017**, *89* (17), 9048–9055. https://doi.org/10.1021/acs.analchem.7b01729.

(14) Nichols, C. M.; Dodds, J. N.; Rose, B. S.; Picache, J. A.; Morris, C. B.; Codreanu, S. G.; May, J. C.; Sherrod, S. D.; McLean, J. A. Untargeted Molecular Discovery in Primary Metabolism: Collision Cross Section as a Molecular Descriptor in Ion Mobility-Mass Spectrometry. *Anal. Chem.* **2018**, *90* (24), 14484–14492. https://doi.org/10.1021/acs.analchem.8b04322.

(15) Maciejewski, M. W.; Schuyler, A. D.; Gryk, M. R.; Moraru, I. I.; Romero, P. R.; Ulrich, E. L.; Eghbalnia, H. R.; Livny, M.; Delaglio, F.; Hoch, J. C. NMRbox: A Resource for Biomolecular NMR Computation. *Biophys. J.* **2017**, *112* (8), 1529–1534. https://doi.org/10.1016/j.bpj.2017.03.011.

(16) Castañar, L.; Poggetto, G. D.; Colbourne, A. A.; Morris, G. A.; Nilsson, M. The GNAT: A New Tool for Processing NMR Data. *Magn. Reson. Chem.* **2018**, *56* (6), 546–558. https://doi.org/10.1002/mrc.4717.

(17) Stejskal, E. O.; Tanner, J. E. Spin Diffusion Measurements: Spin Echoes in the Presence of a Time-Dependent Field Gradient. *J. Chem. Phys.* **1965**, *42* (1), 288–292. https://doi.org/10.1063/1.1695690.

(18) Sinnaeve, D. The Stejskal-Tanner Equation Generalized for Any Gradient Shape-an Overview of Most Pulse Sequences Measuring Free Diffusion. *Concepts Magn. Reson. Part A* **2012**, *40A* (2), 39–65. https://doi.org/10.1002/cmr.a.21223.

(19) Altenbach., Christian. LongDistances. https://sites.google.com/site/altenbach/labview-programs/epr-programs/long-distances.

(20) Osterby, B. R.; McKelvey, R. D. Convergent Synthesis of Betaine-30, a Solvatochromic Dye: An Advanced Undergraduate Project and Demonstration. *J. Chem. Educ.* **1996**, *73* (3), 260. https://doi.org/10.1021/ed073p260.